SFERA-III

Solar Facilities for the European Research Area

1st Summer School "Thermal energy storage systems, solar fields and new cycles for future CSP plants"
WP1 Capacity building and training activities
Odeillo, France, September 9th-11th 2019

"Raytracing software and design tools for heliostats fields"

Shahab Rohani, Fraunhofer Institute for Solar Energy Systems ISE

NETWORKING

THIS PROJECT HAS RECEIVED FUNDING FROM THE EUROPEAN UNION'S HORIZON 2020 RESEARCH AND INNOVATION PROGRAMME UNDER GRANT AGREEMENT NO **823802**

RAYTRACING SOFTWARE AND DESIGN TOOLS FOR HELIOSTATS FIELDS

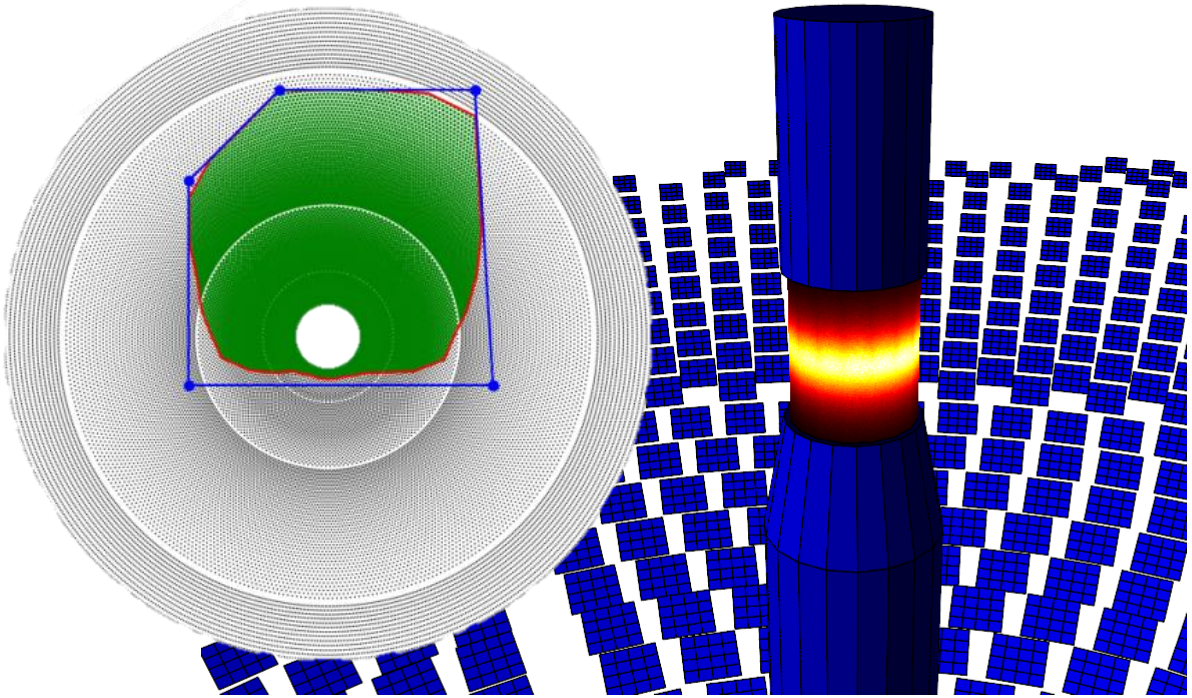

Shahab Rohani, Peter Schöttl

Fraunhofer Institute for Solar Energy Systems ISE

SFERA III Summer School

Odeillo, Sep. 9-11 2019

www.ise.fraunhofer.de

AGENDA

- Raytrace3D
  - Basics
  - Simulation acceleration
  - Angle-dependent reflectance for soiling modeling
  - Individual heliostat assessment
  - Sky discretization for fast annual assessment
  - Coupling to dynamic receiver simulation
- Heliostat field design/optimization
  - Heliostat field layout algorithms
  - Heliostat selection based on polygon optimization

Raytrace3D
Principle

Monte-Carlo forward ray tracing

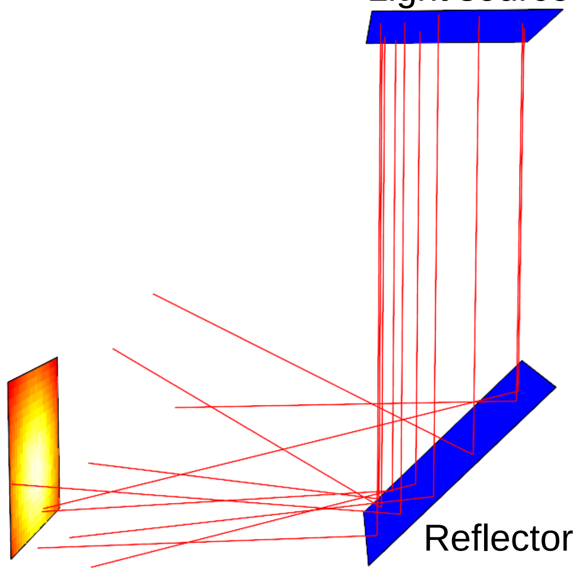

Features

- Comprehensive library of geometries/materials/light sources
  ➔ sophisticated modeling of solar applications
- Fully object-oriented
  ➔ readily extensible
- Number crunching in C++
  + Pre/Postprocessing in Python
  ➔ Fast and versatile
- Parallelized
  ➔ Run on simulation servers

Raytrace3D

Heliostat field losses

- Monte-Carlo ray tracing:
  Fraunhofer ISE tool *Raytrace3D*
  - Cosine losses
  - Shading
  - Absorption on heliostats
  - Blocking
  - Atmospheric attenuation
  - Spillage
  - Reflection from receiver
- Flux distribution
  on receiver surfaces [1]

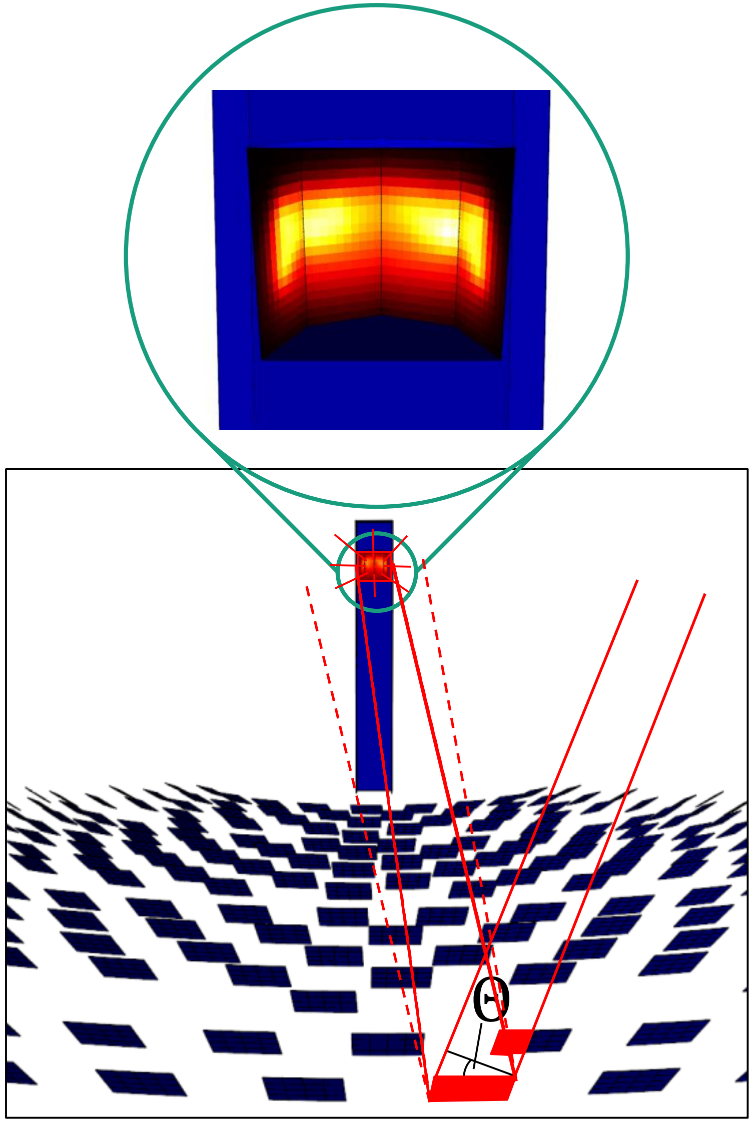

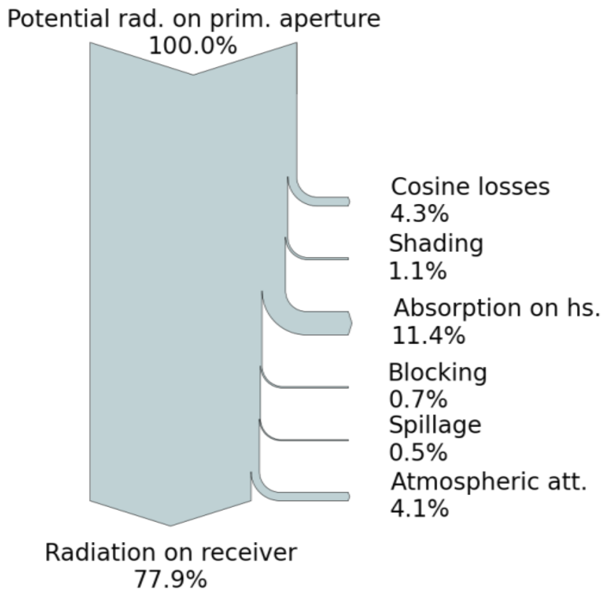

[1] P. Schöttl, G. Bern, D. W. van Rooyen, J. Flesch, T. Fluri, and P. Nitz, “Efficient modeling of variable solar flux distribution on Solar Tower receivers by interpolation of few discrete representations,” Solar Energy, vol. 160, pp. 43–55, 2018.

Raytrace3D
Graphical postprocessing

Gemasolar system
Fluxmaps depicted on receiver surfaces

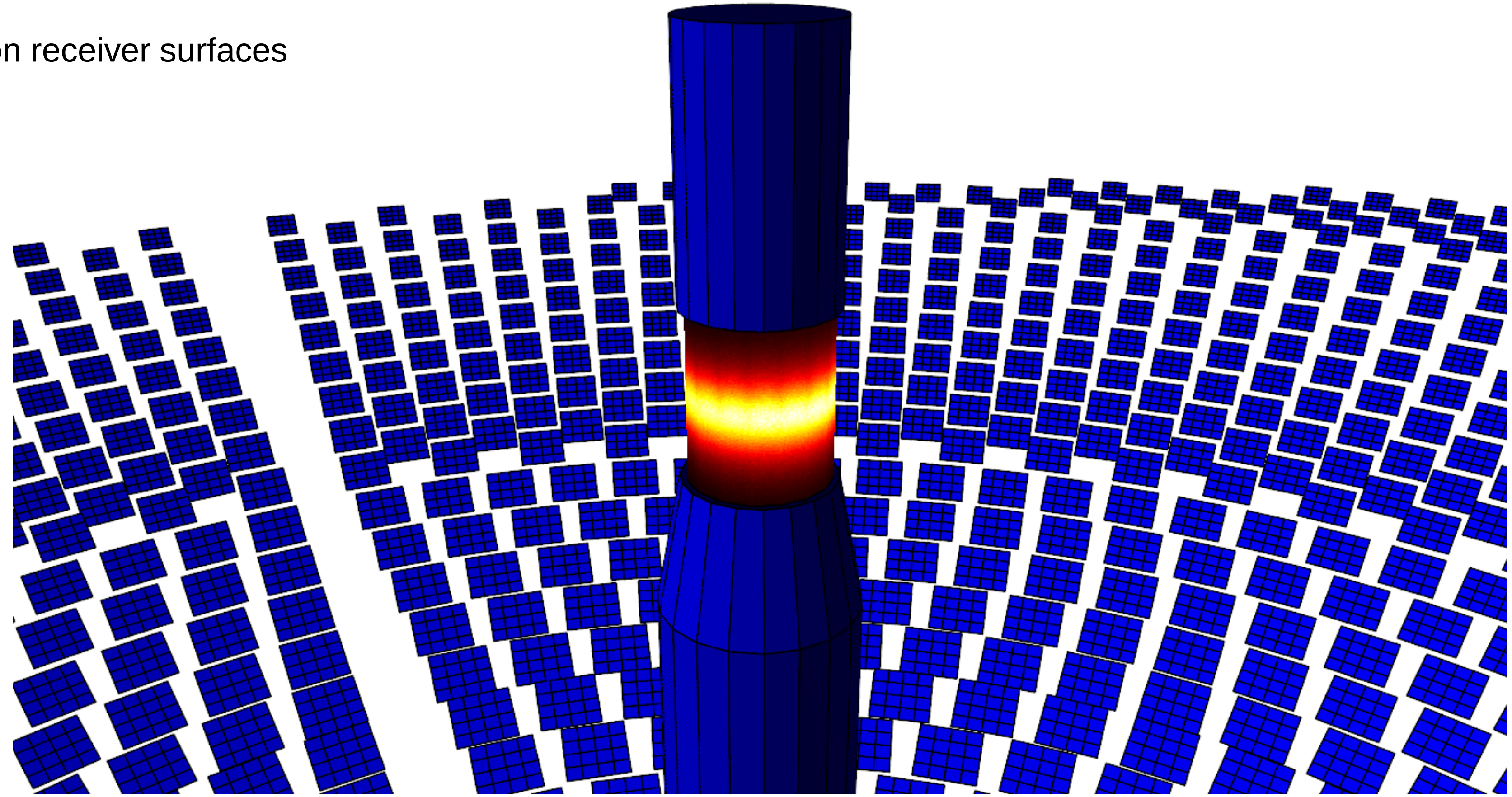

Raytrace3D

Simulation of solar towers

Solar Two

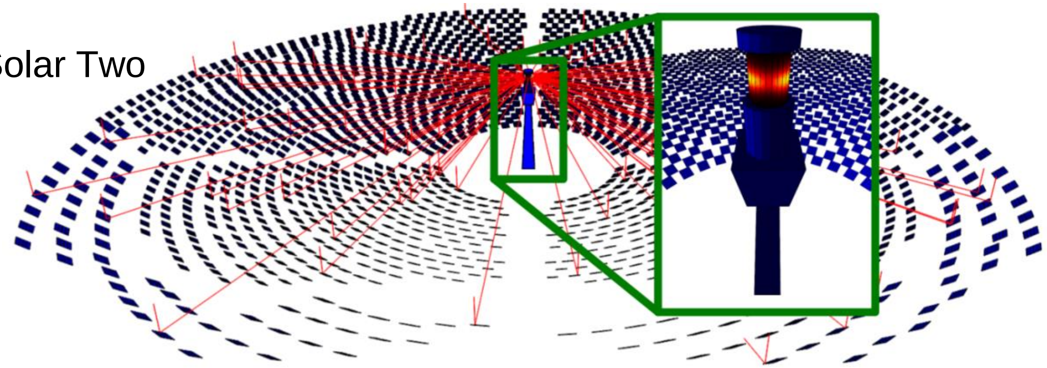

Gemasolar

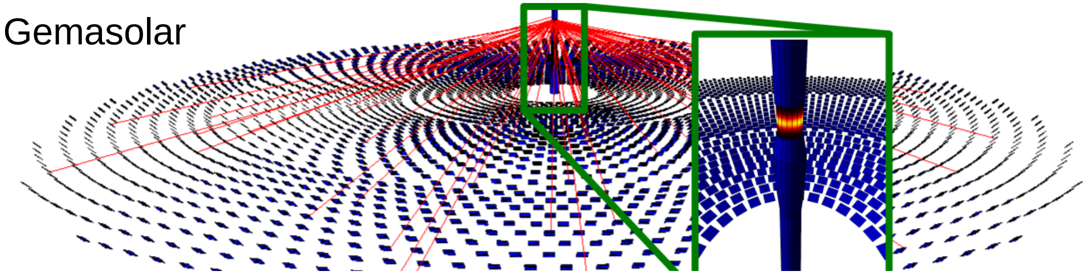

PS10

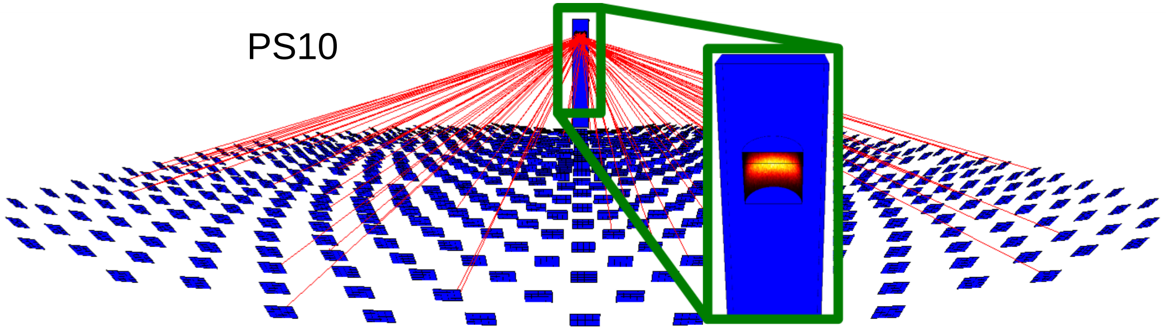

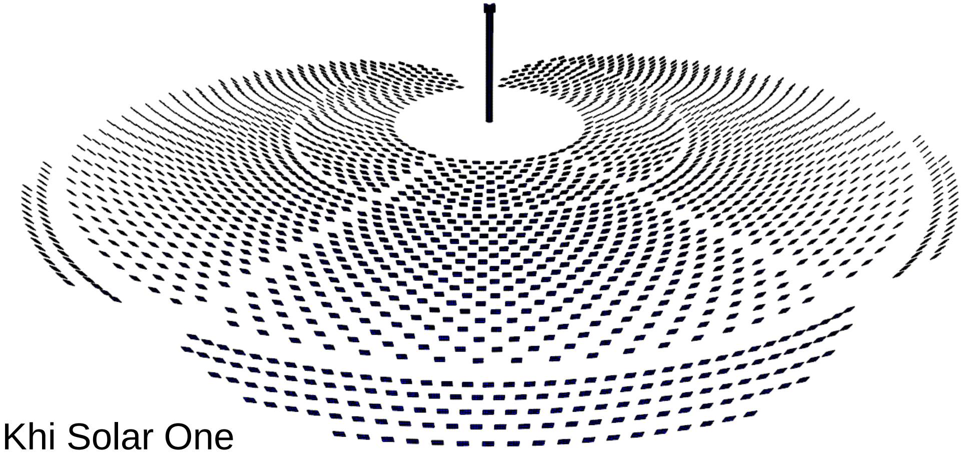

Ivanpah

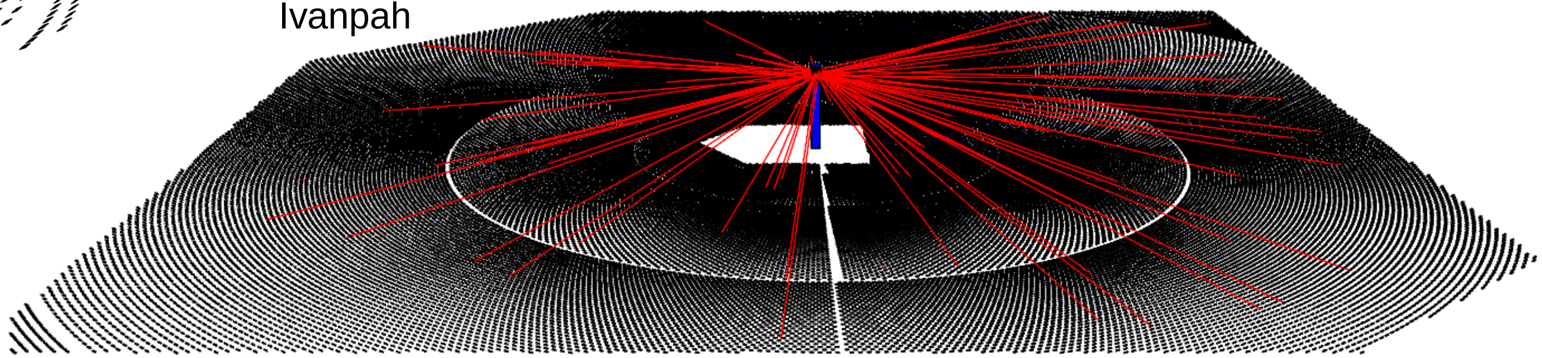

Khi Solar One

Raytrace3D concepts
Angle-dependent reflectance for soiling modeling

- Clean mirrors → weak incidence angle dependency of reflectance
- Soiled mirrors → strong incidence angle dependency of reflectance

- Raytrace3D: incidence angle dependent reduction of reflectance
- Reduction of solar yield

➢ Improved yield prediction

➢ Optimization of cleaning cycles

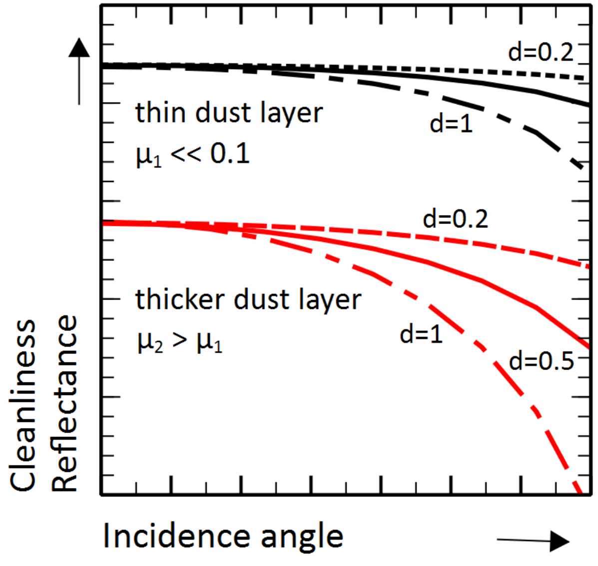

[2]

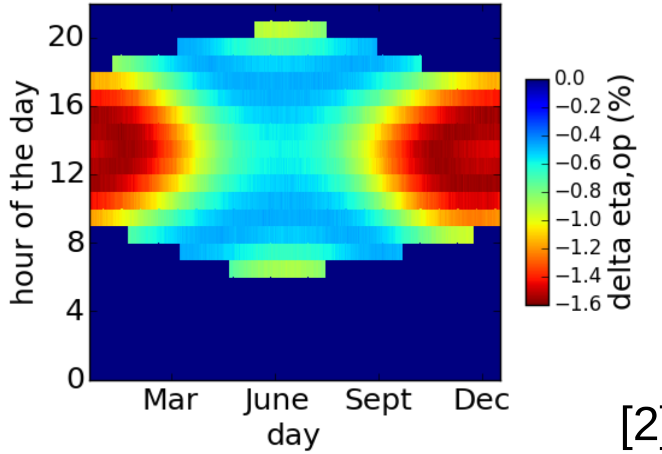

[2]

[2] A. Heimsath, P. Nitz, The effect of soiling on the reflectance of solar reflector materials - Model for prediction of incidence angle dependent reflectance and attenuation due to dust deposition, Solar Energy Materials and Solar Cells, vol. 195,pp 258-268, , 2019

Fraunhofer ISE

Raytrace3D concepts
Individual heliostat assessment

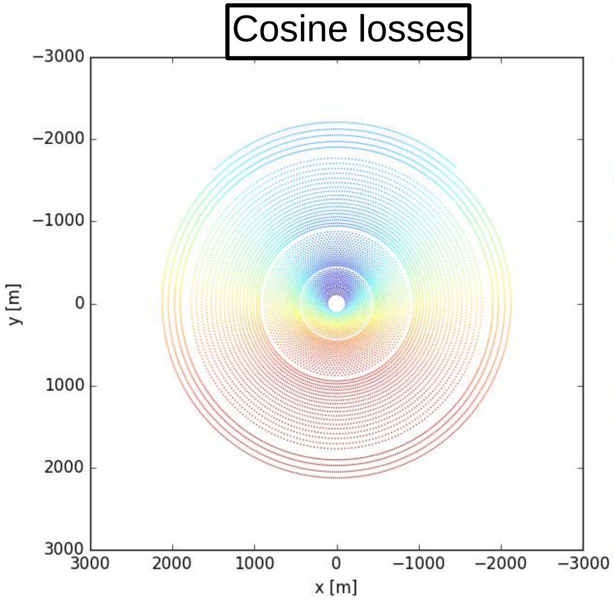

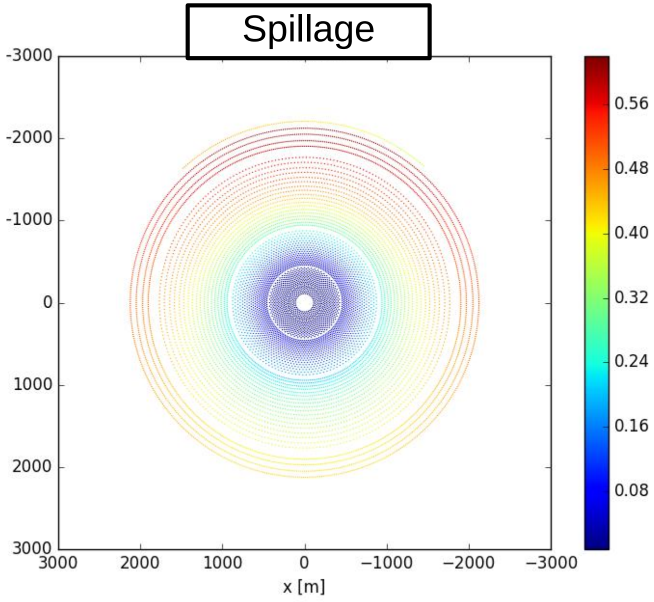

- Built-in routine for evaluating ray history
- Per-unit assessment of primary aperture (heliostats)
- Evaluation of different loss mechanisms (cos shading, …)
- (Optional) integration of secondary concentrator

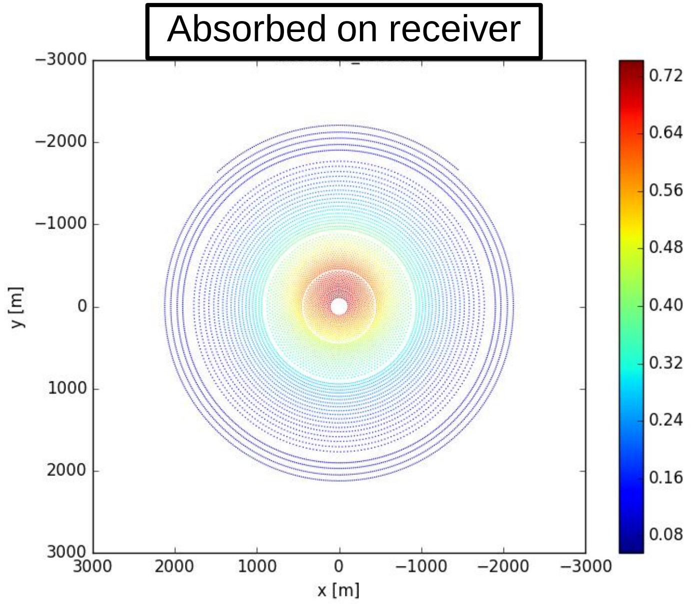

➢ Full insight in heliostat field loss mechanisms

➢ Input for field design

Fraunhofer ISE

Raytrace3D concepts

Sky discretization for fast annual assessment [2,3]

- Uniform discretization of the sky hemisphere

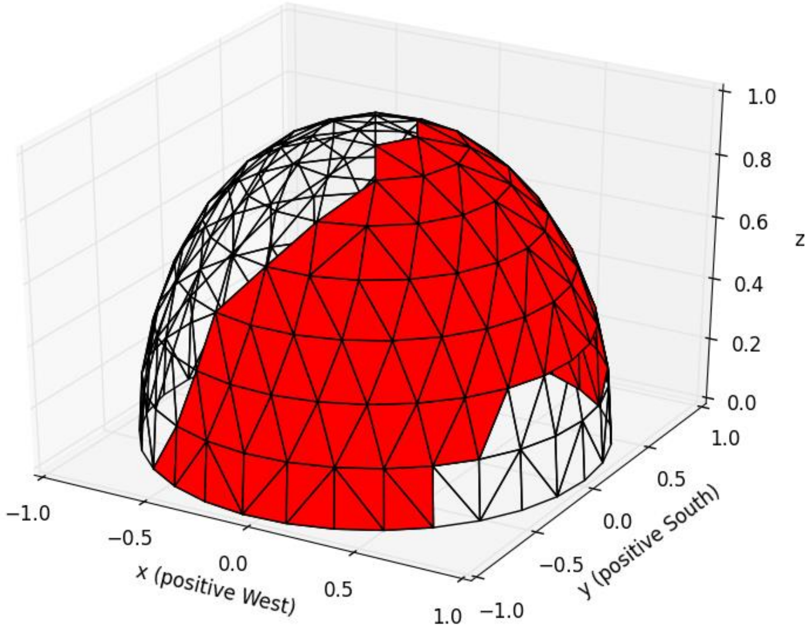

[3] P. Schöttl, G. Bern, D. W. van Rooyen, J. Flesch, T. Fluri, and P. Nitz, “Efficient modeling of variable solar flux distribution on Solar Tower receivers by interpolation of few discrete representations,” Solar Energy, vol. 160, pp. 43–55, 2018.
[4] P. Schöttl, K. Ordóñez Moreno, F. C. D. van Rooyen, G. Bern, and P. Nitz, “Novel sky discretization method for optical annual assessment of solar tower plants,” Solar Energy, vol. 138, pp. 36–46, 2016.

Raytrace3D concepts

Sky discretization for fast annual assessment [2,3]

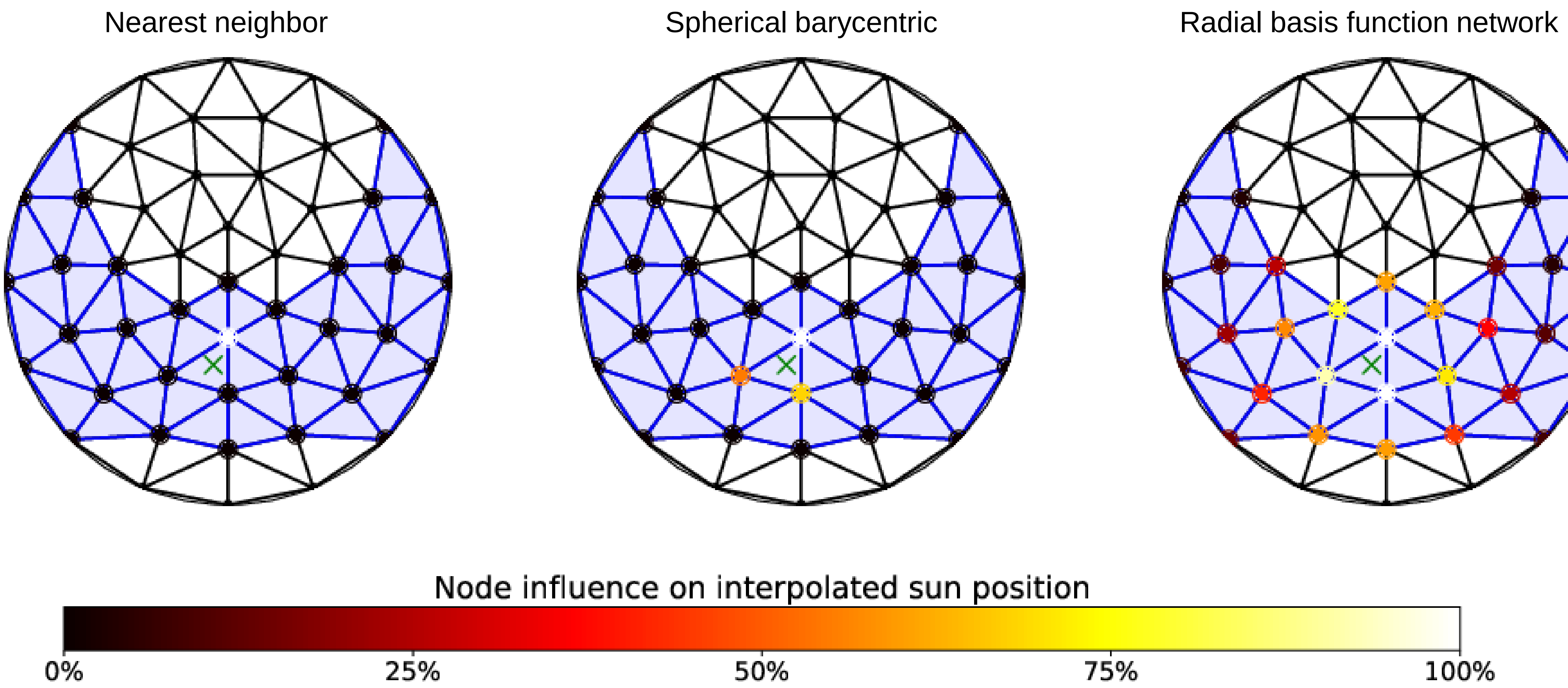

[3] P. Schöttl, G. Bern, D. W. van Rooyen, J. Flesch, T. Fluri, and P. Nitz, “Efficient modeling of variable solar flux distribution on Solar Tower receivers by interpolation of few discrete representations,” Solar Energy, vol. 160, pp. 43–55, 2018.
[4] P. Schöttl, K. Ordóñez Moreno, F. C. D. van Rooyen, G. Bern, and P. Nitz, “Novel sky discretization method for optical annual assessment of solar tower plants,” Solar Energy, vol. 138, pp. 36–46, 2016.

Fraunhofer ISE

Raytrace3D concepts

Coupling to dynamic receiver simulation

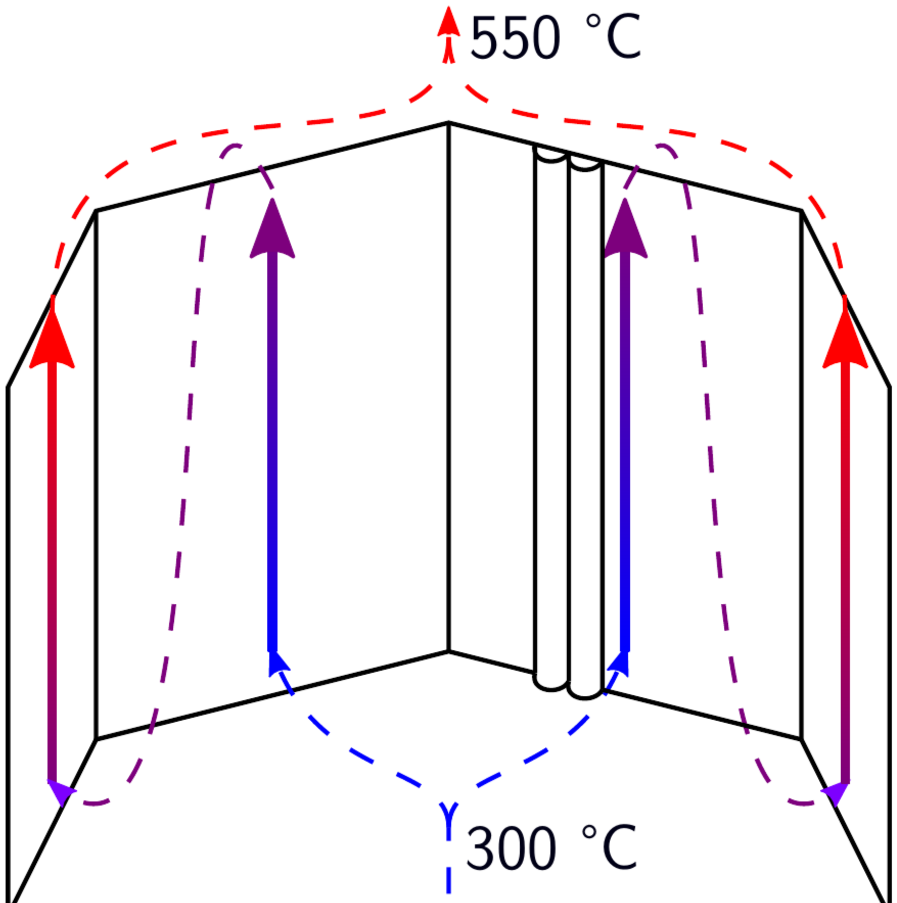

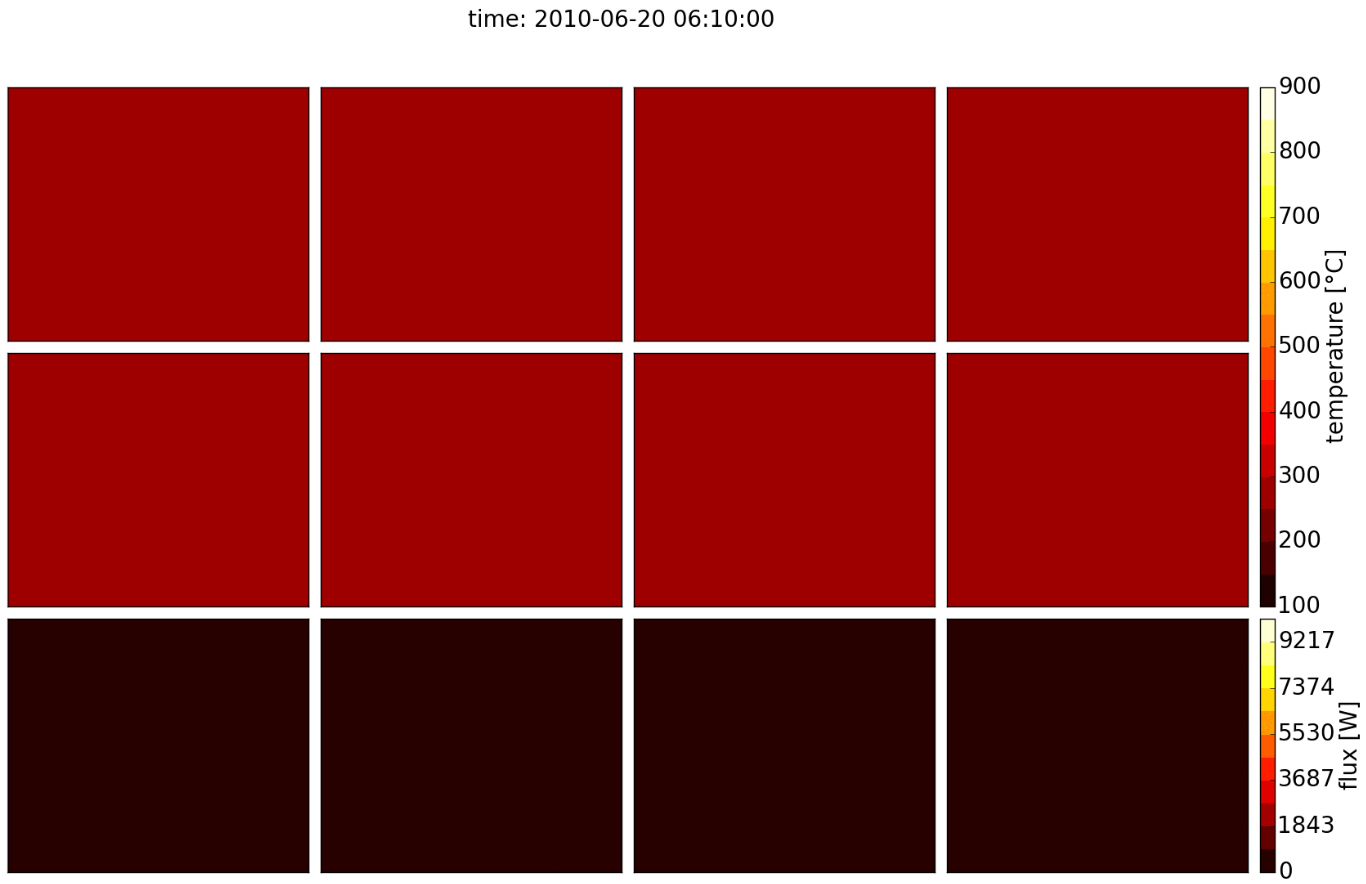

Top row: Temperature distribution [°C] in the fluid
Center row: Temperature distribution [°C] on the panel surface
Bottom row: Flux distribution [W] on the panel surface

AGENDA

- Raytrace3D
  - Basics
  - Simulation acceleration
  - Angle-dependent reflectance for soiling modeling
  - Individual heliostat assessment
  - Sky discretization for fast annual assessment
  - Coupling to dynamic receiver simulation
- Heliostat field design/optimization
  - Heliostat field layout algorithms
  - Heliostat selection based on polygon optimization

Heliostat field design/optimization
Patterns-based algorithms

- Layout algorithms based on underlying pattern
- Base cases: radially staggered vs. cornfield
- Several free parameters
- Advantages:
  - Fast creation of large fields
  - Construction and maintenance easier in a regular layout
- Disadvantage:
  - Difficult to adapt to uneven terrain

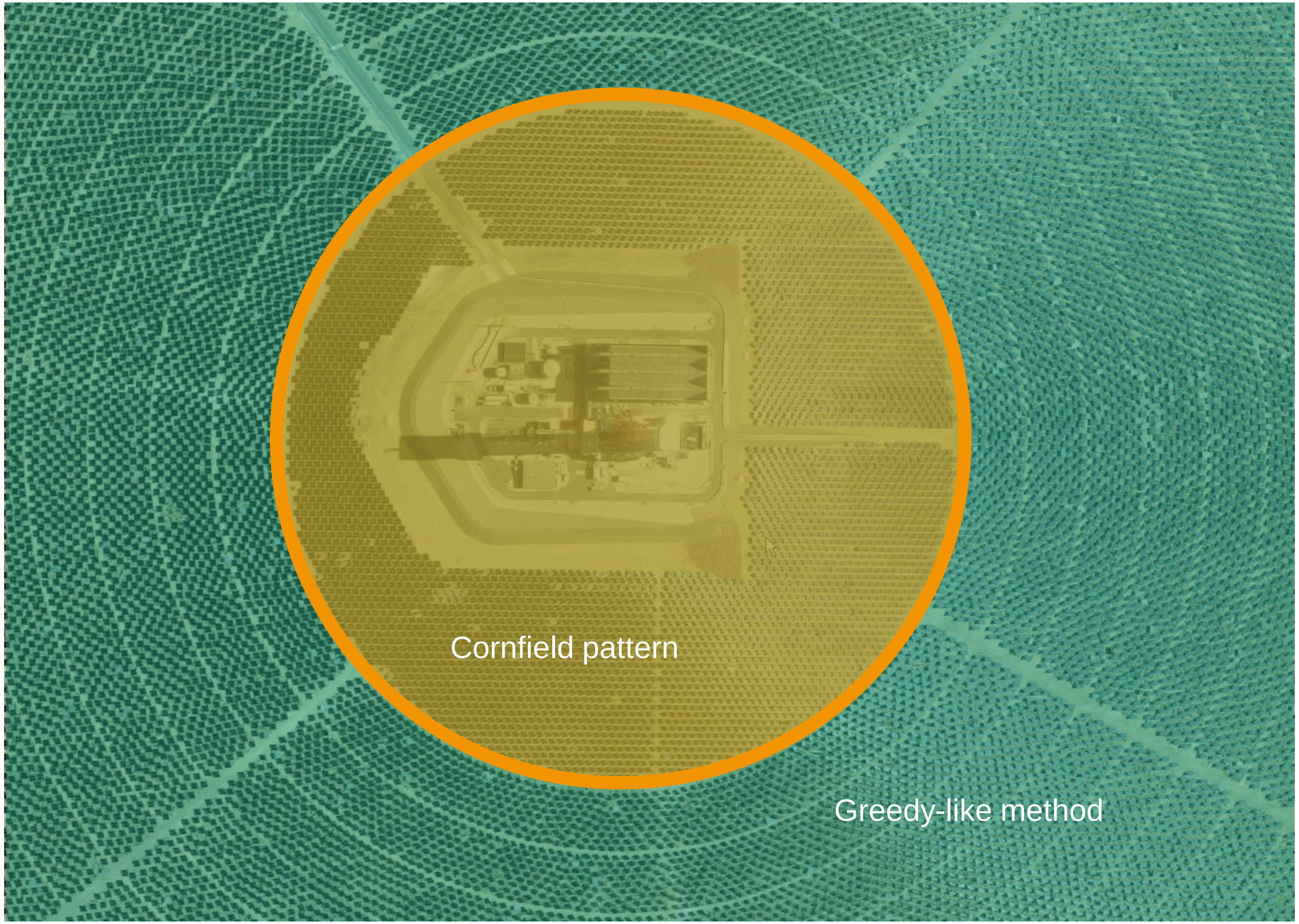

Part of Ivanpah field (source: Google Maps)

Heliostat field design/optimization
MUEEN layout

- Aim: no blocking
- Radially staggered
- Re-grouping for denser field
- Original algorithm [6] extended by Fraunhofer ISE [5]

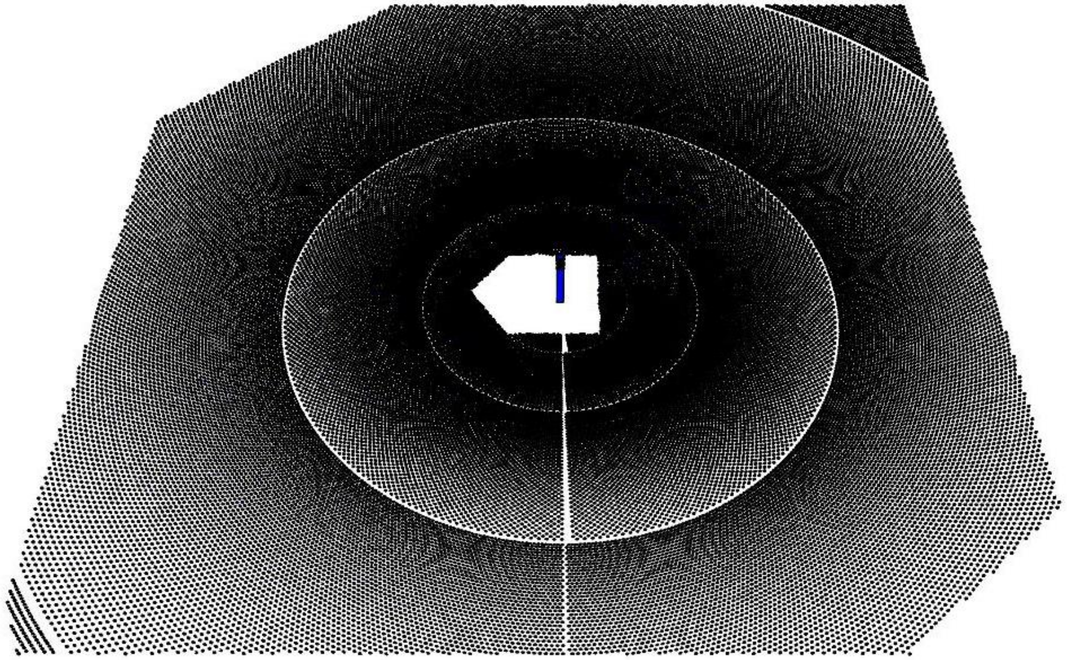

Re-modeling of Ivanpah heliostat field with *Fraunhofer ISE MUEEN* algorithm and field boundaries

[5] F.M.F. Siala and M.E. Elayeb, “Mathematical formulation of a graphical method for a no-blocking heliostat field layout,” Renewable Energy, vol. 23, no. 1, pp. 77–92, http://linkinghub.elsevier.com/retrieve/pii/S0960148100001592, 2001.
[6] E. Leonardi, L. Pisani, I. Les, A. Mutuberria, S. Rohani, and P. Schöttl, “Techno-Economic Heliostat Field Optimization: Comparative Analysis of Different Layouts,” Solar Energy, vol. 180, pp. 601–607, 2019.

Heliostat field design/optimization
CAMPO layout [7]

- Radially staggered
- Creation of densest possible field
- Azimuthal and radial stretching (local!) to reduce shading and blocking

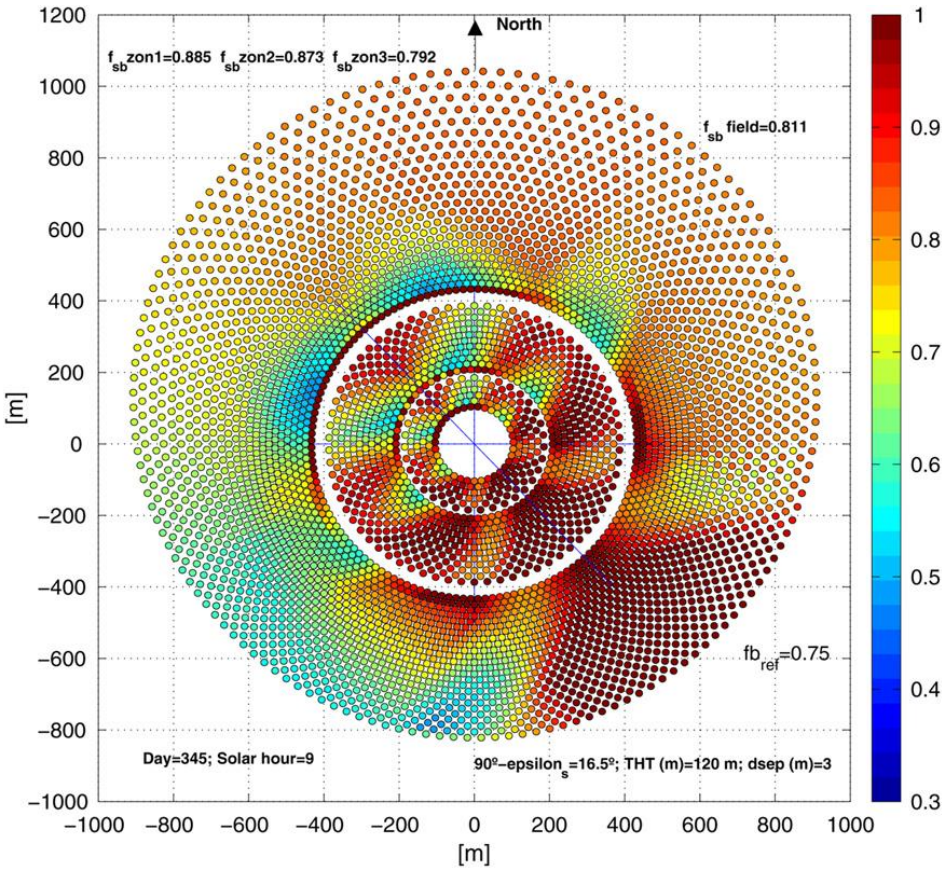

Field generated with CAMPO algorithm (plot from [7])

[7] F. J. Collado and J. Guallar, “Campo: Generation of regular heliostat fields,” Renewable Energy, vol. 46, no. 0, pp. 49–59, http://www.sciencedirect.com/science/article/pii/S096014811200198X, 2012.

Heliostat field design/optimization
Biomimetic layout [8]

- Biomimetic phylotaxis disc pattern
  ➔ sunflower
- Angular distribution is related to the golden ratio
  $(1+\sqrt{5})/2$
- Optimization of free parameter

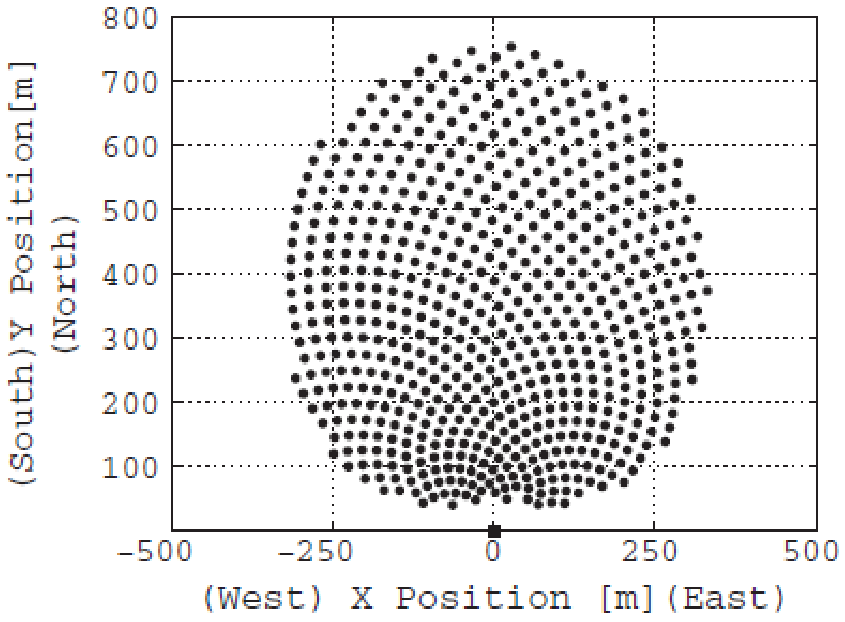

Field generated with biomimetic algorithm (plot from [8])

[8] C. J. Noone, M. Torrilhon, and A. Mitsos, "Heliostat field optimization: A new computationally efficient model and biomimetic layout," Sol Energy, vol. 86, no. 2, pp. 792–803, http://www.sciencedirect.com/science/article/pii/S0038092X11004373, 2012.

Heliostat field design/optimization
Pattern-free algorithms

- No underlying pattern
- Heliostat placement based on some heuristic
- Advantages:
  - Easily applicable to uneven terrain
- Disadvantage:
  - Field creation very complicated and computationally intensive

Heliostat field design/optimization
Genetic algorithm [9]

- Random generation of initial heliostat base points
- Genetic algorithm (cross-over, mutation, selection) to optimize field

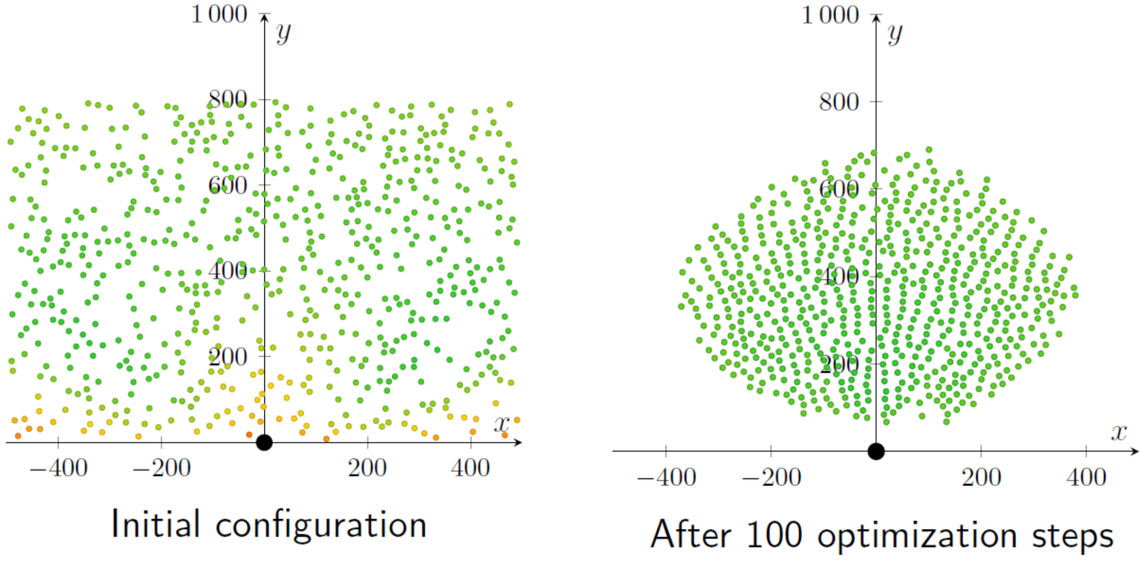

Field optimization with genetic algorithm (plot from presentation related to [9])

[9] P. Richter, M. Frank, and E. Abraham, "Multi-objective optimization of solar tower heliostat fields," in Proceedings of European Conference on Mathematics for Industry (ECMI 2014), 2014.

Heliostat field design/optimization

Greedy algorithm [10]

- Iterative growth of the heliostat field
- Every new heliostat is placed at the currently best position in the available area
- Different implementations available

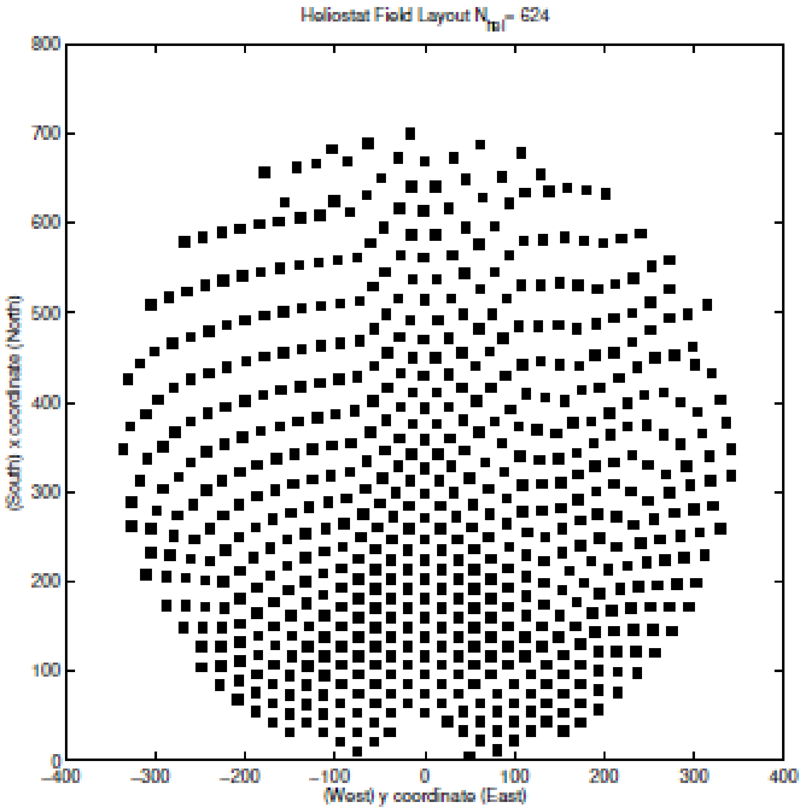

Field optimization with greedy algorithm (plot from [10])

[10] E. Carrizosa, C. Domínguez-Bravo, E. Fernández-Cara, and M. Quero, "A heuristic method for simultaneous tower and pattern-free field optimization on solar power systems," Computers & Operations Research, vol. 57, no. 0, pp. 109–122, http://www.sciencedirect.com/science/article/pii/S0305054814003219, 2015.

HELIOSTAT SELECTION BASED ON POLYGON OPTIMIZATION

- Motivation
- Problem Description
- Methodology
- Application
- Summary & Outlook

Motivation

- Heliostat field represents about 40% of CAPEX of entire plant [1]
- Typical loss composition for a 600 MW_{th} Solar Tower plant [3]

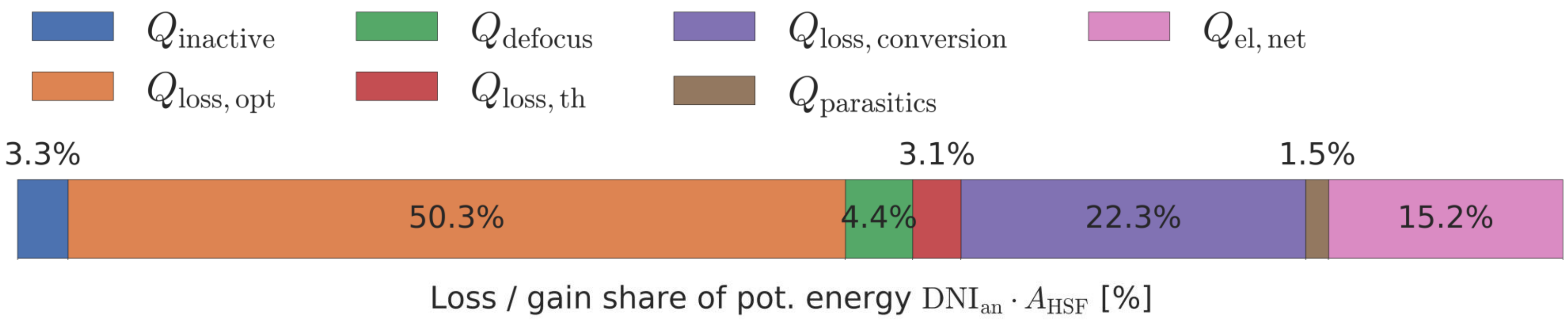

➢ Field design for **high annual efficiency** and **low cost** is crucial

[1] IRENA, “Renewable energy technologies: Cost Analysis Series - Concentrating Solar Power,” 2012.

[3] Schöttl et al., “Performance Assessment of a Secondary Concentrator for Solar Tower External Receivers,” submitted to 24th SolarPACES Conference, 2 – 5 October 2018, Casablanca, Morocco.

Heliostat selection based on polygon optimization

Problem description: Heliostat Selection from Oversized Field

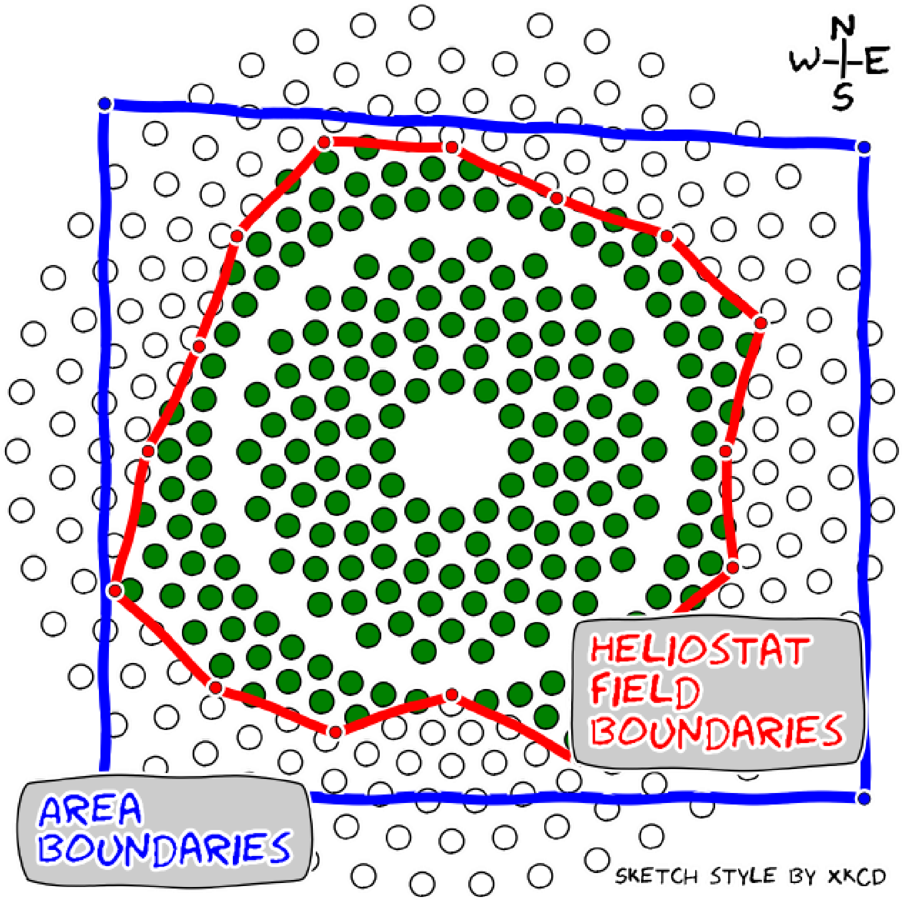

- Respect area boundaries
- Meet flux requirements
- Optimize for given objective function
- Coherent field, feasible w.r.t. construction and maintenance

HELIOSTAT SELECTION BASED ON POLYGON OPTIMIZATION

- Problem Description
- Methodology
  - Oversized Field
  - Polygon-Based Selection
  - Area Boundaries
  - Evolutionary Optimization Algorithm
- Application
- Summary & Outlook

Methodology
Oversized Field

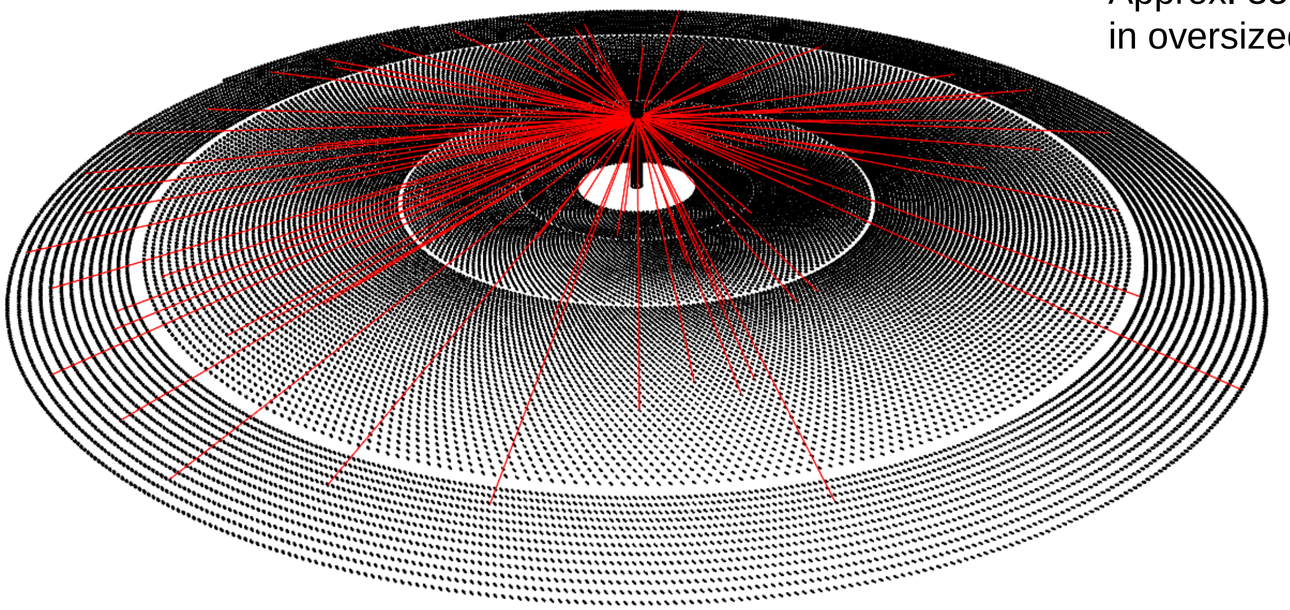

Approx. 35k heliostats
in oversized field

- Generation with **extended MUEEN algorithm [4]**
- Assessment with **Raytrace3D [5**

[4] Siala and Elayeb, “Mathematical formulation of a graphical method for a no-blocking heliostat field layout,” 2001.

[5] Branke and Heimsath, “Raytrace3D-Power Tower - A Novel Optical Model For Central Receiver Systems,” 2010.

Methodology
Polygon-Based Selection

- Equi-angular vertices
- Centered around tower base

- Only vertex radii as free parameters in optimization
- Coherent field boundaries
- Evaluation of objective function

  on entire field

- For polar field, limit angular range

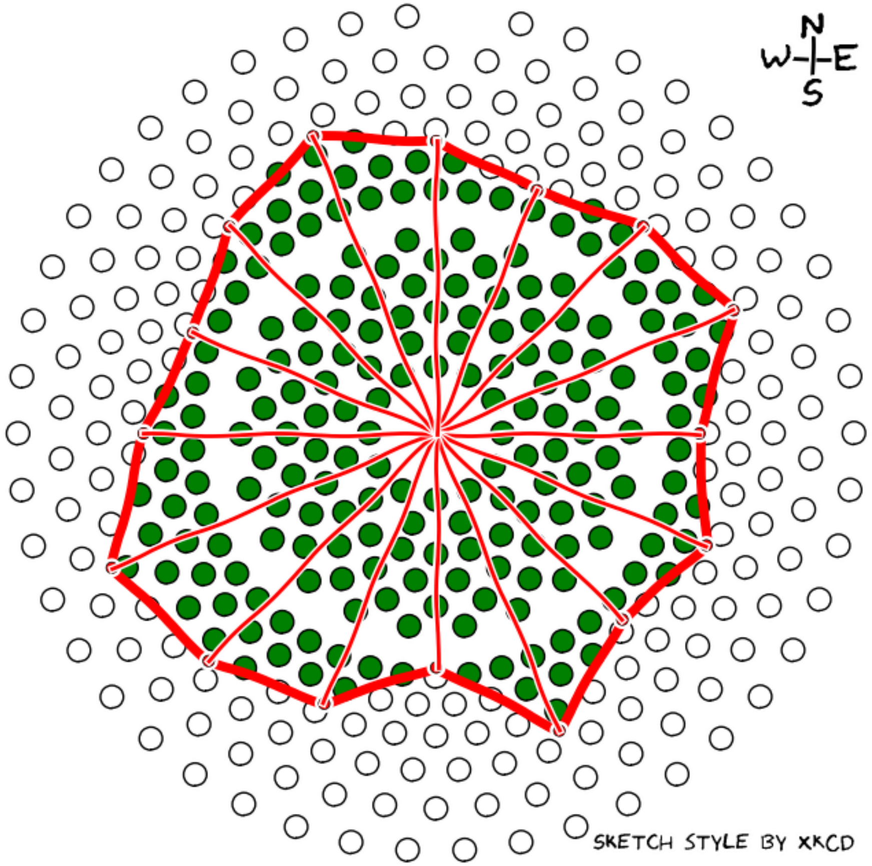

Methodology
Area Boundaries

- Yet another polygon
- Move relative to tower base
- ➢ Two additional degrees of freedom: Δx, Δy

Area boundaries are

- ~~Large, not constraining~~
- Large enough, constraining
- ~~Too small~~

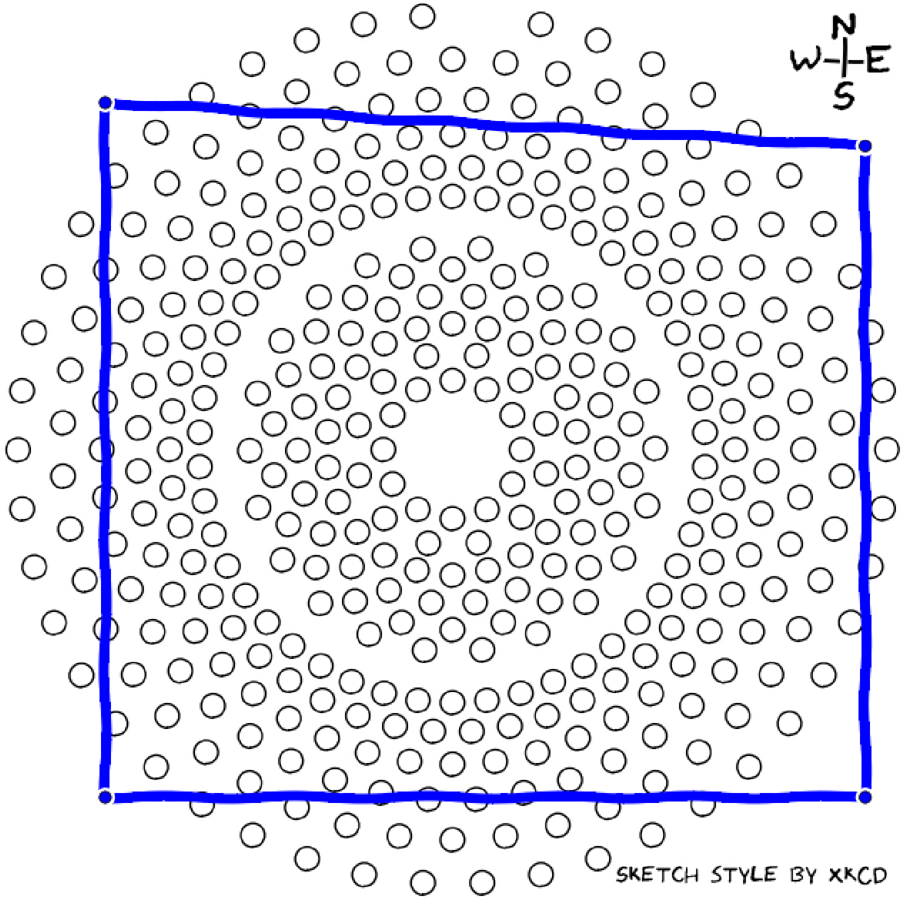

Methodology

Evolutionary Optimization Algorithm

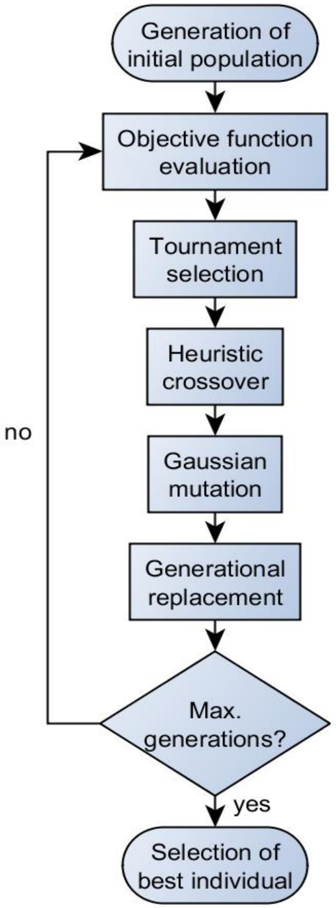

Problem-specific tweaks

- Penalty on not reaching required flux at design point
- Mutation range decreases with sigmoid function

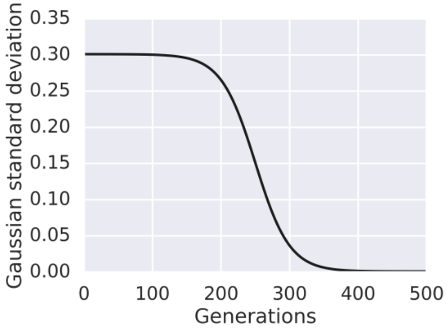

- Small tournament size of 3
- Full generational replacement, no elitism

➢ low selection pressure, no premature convergence

HELIOSTAT SELECTION BASED ON POLYGON OPTIMIZATION

- Problem Description
- Methodology
- Application
  - Base Scenario
  - Objective Function
  - Examples
- Summary & Outlook

Application
Base Scenario

Parameter	Value [6]
Site	Seville, Spain
Absorbed power at design point	55.27 MW
Tower height	100.5 m
External receiver diameter	14 m
External receiver height	12 m
Number of heliostats in oversized field	35000
Heliostat area (square)	8 m²
Minimum radial heliostat distance to tower	80 m
Design point	Winter solstice
Design DNI	850 W/m²

[6] Leonardi et al., “Techno-Economic Heliostat Field Optimization: Comparative Analysis of Different Layouts,” Submitted to Solar Energy Journal, 2018.

Application
Objective function

Objective function maximizes yield per cost [6]:

- annual optical efficiency η_{an} of the entire field
- ground area A_{ground} being the convex hull of all heliostats
- cumulative mirror area A_{HSF} of all heliostats
- cost ratio $k = \frac{k_{ground}}{k_{HSF}}$ of ground area to mirror area
- Cumulative annual direct normal irradiance DNI_{an}

[6] Leonardi et al., “Techno-Economic Heliostat Field Optimization: Comparative Analysis of Different Layouts,” Submitted to Solar Energy Journal, 2018.

Application

No Area Boundaries, Cost Ratio k=0%

$$OF = \frac{\eta_{an}}{k \cdot \frac{A_{ground}}{A_{HSF}} + 1} = \eta_{an}$$

Animations showing best candidate every ten generations

Application
No Area Boundaries, Cost Ratio k=0%

$$OF = \eta_{an}$$

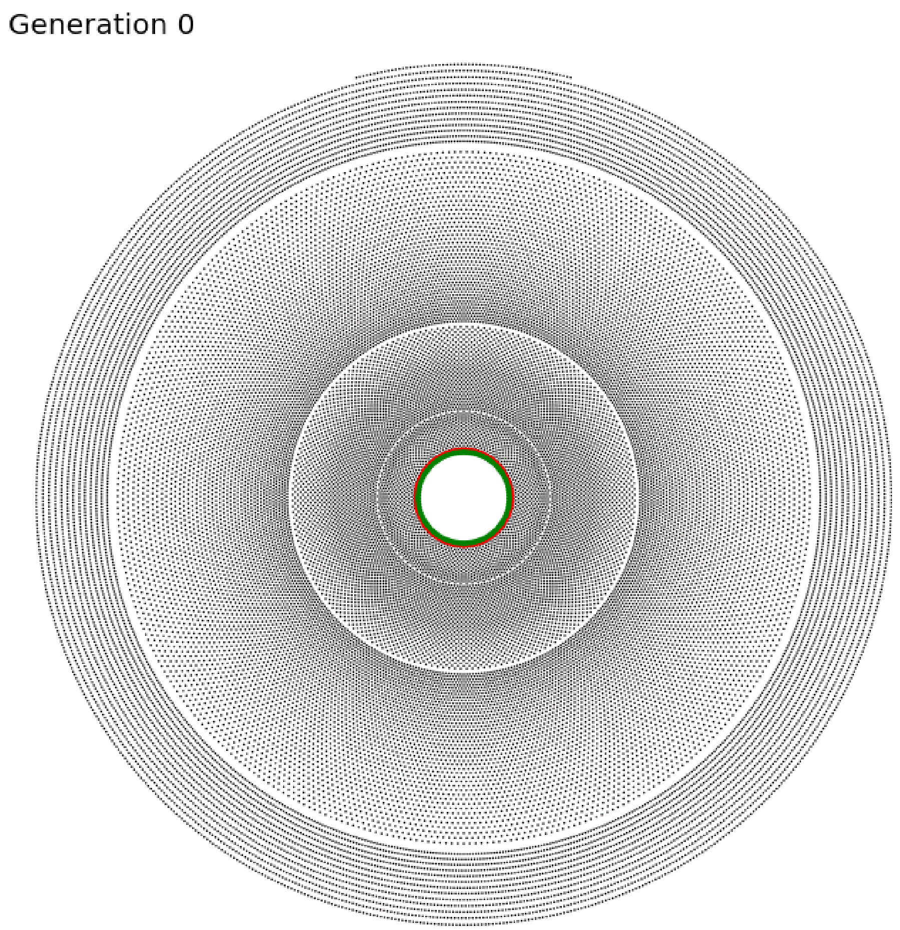

Application

No Area Boundaries, Cost Ratio k=0%

$$OF = \eta_{an}$$

G 10

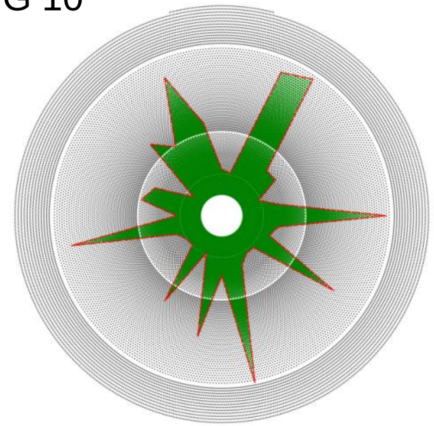

G 100

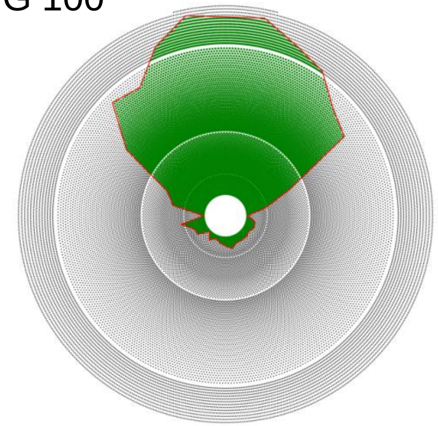

G 200

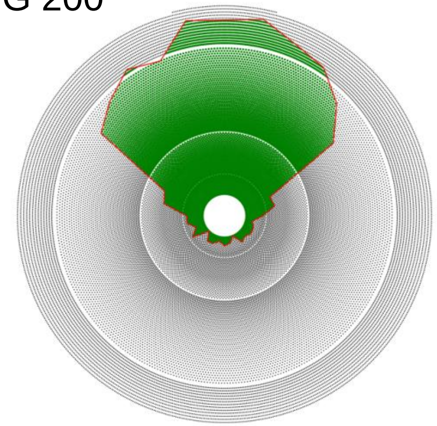

G 300

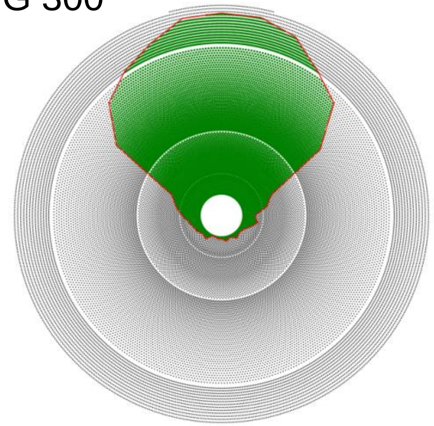

G 400

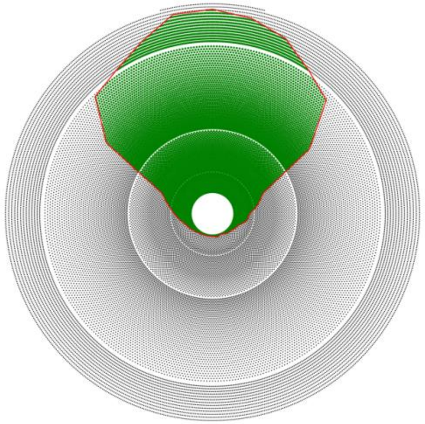

G 500

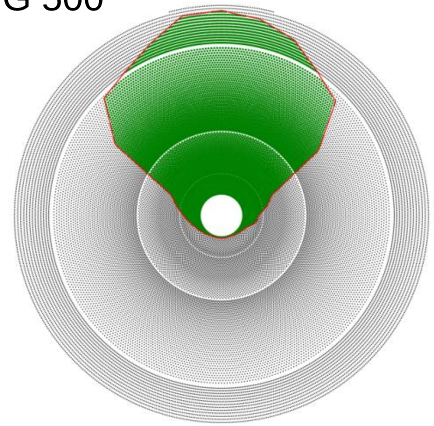

Application

No Area Boundaries, Cost Ratio k=4%

$$OF = \frac{\eta_{an}}{k \cdot \frac{A_{ground}}{A_{HSF}} + 1}$$

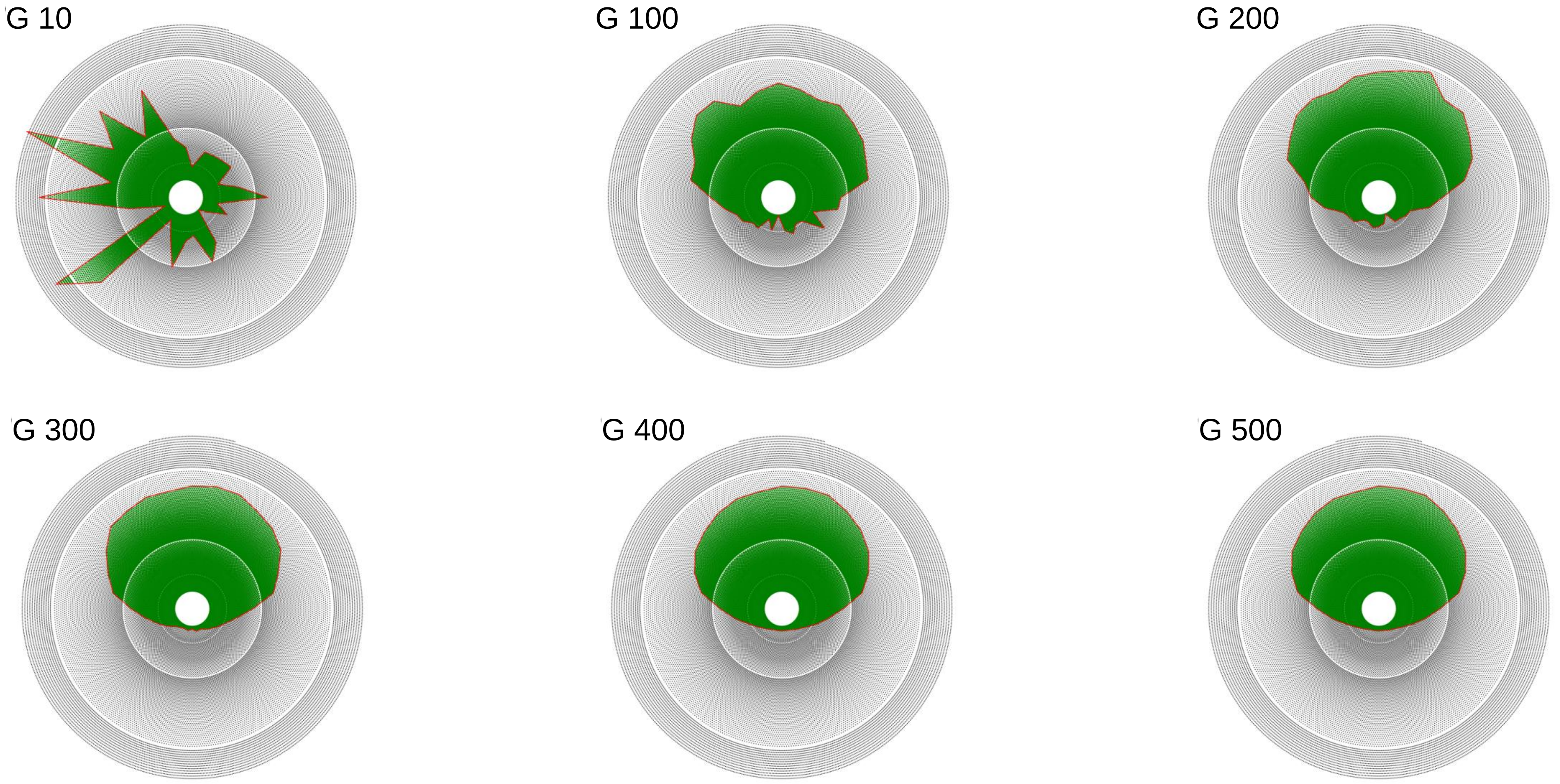

Application

Complex Area Constraints, Cost Ratio k=0%

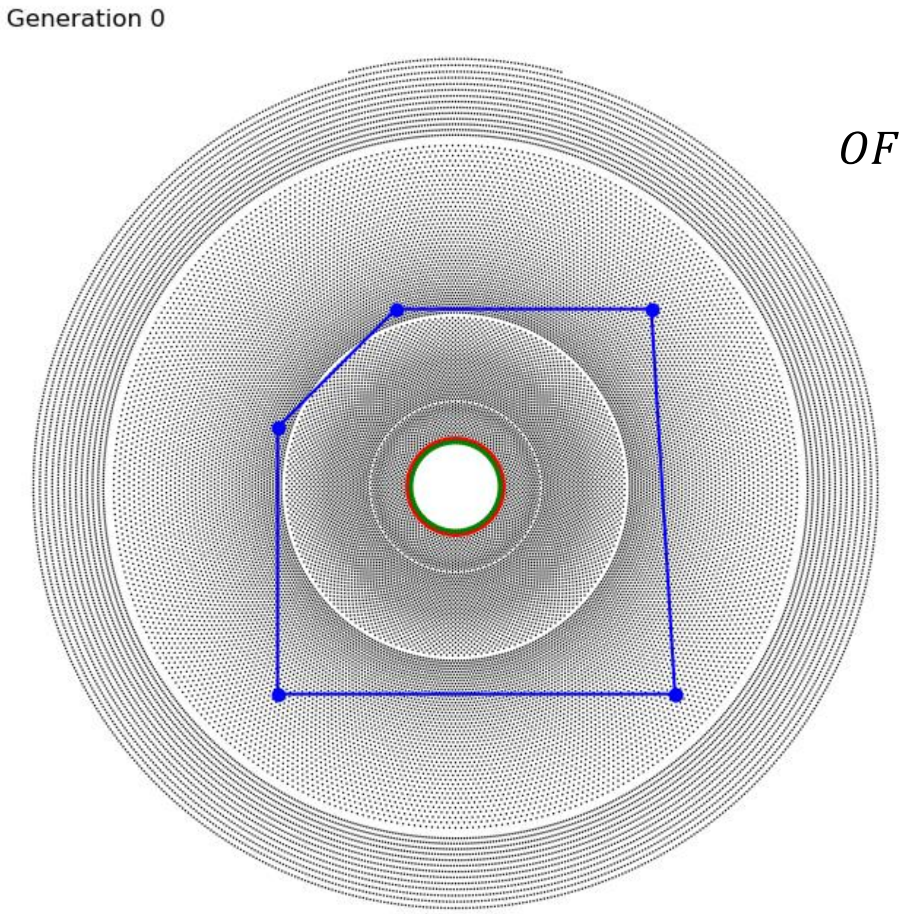

$$OF = \frac{\eta_{an}}{k \cdot \frac{A_{ground}}{A_{HSF}} + 1} = \eta_{an}$$

Application

Complex Area Constraints, Cost Ratio k=0%

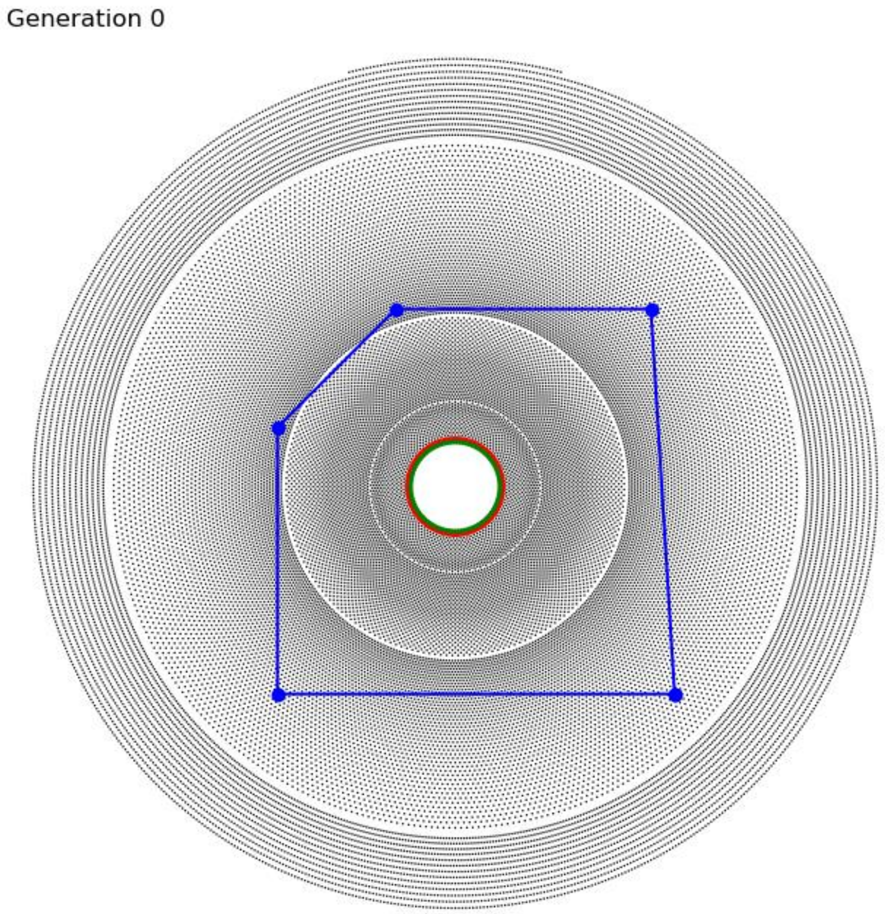

$$OF = \eta_{an}$$

Application

Complex Area Constraints, Cost Ratio k=0%

$$OF = \eta_{an}$$

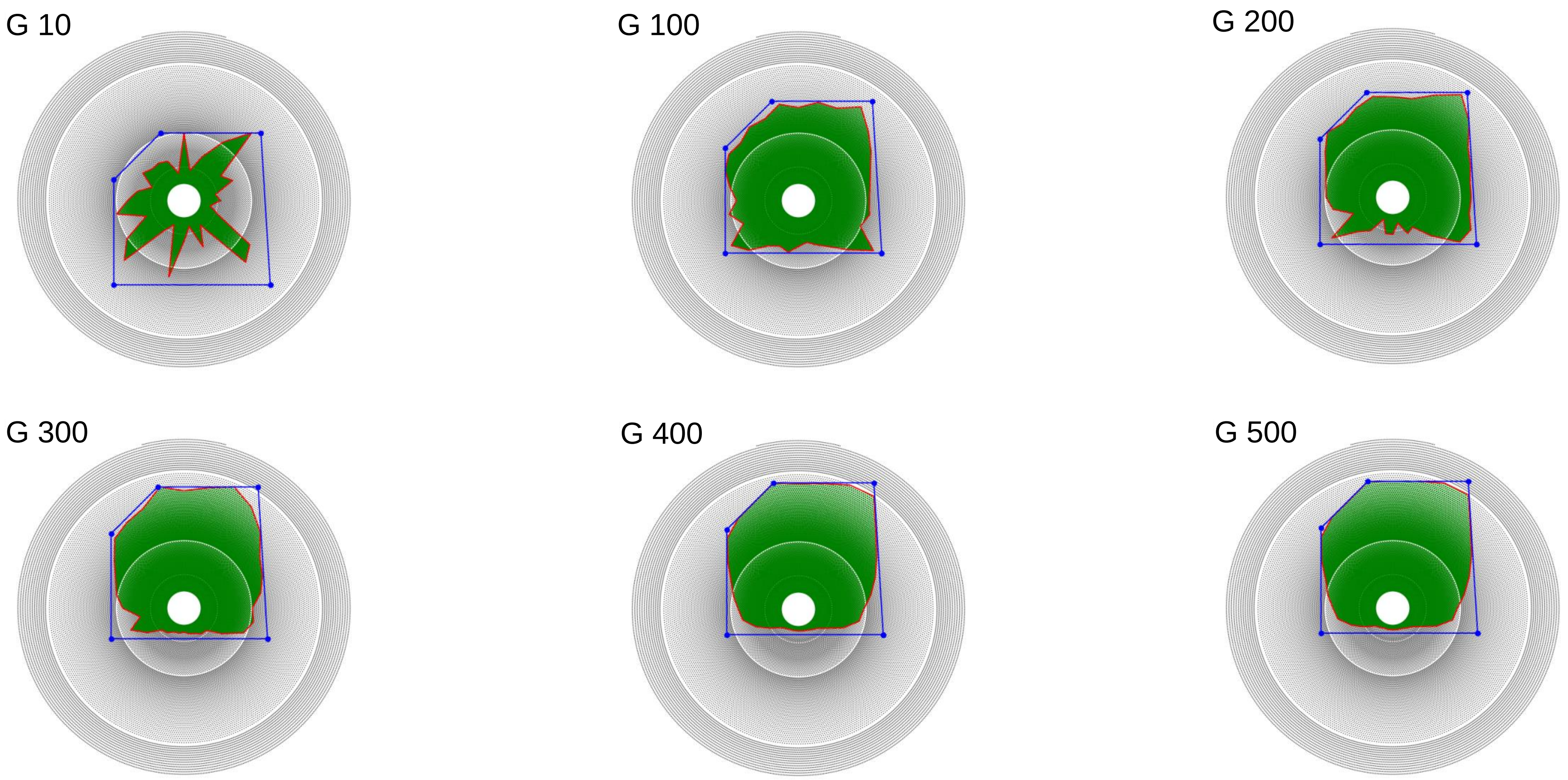

Summary & Outlook

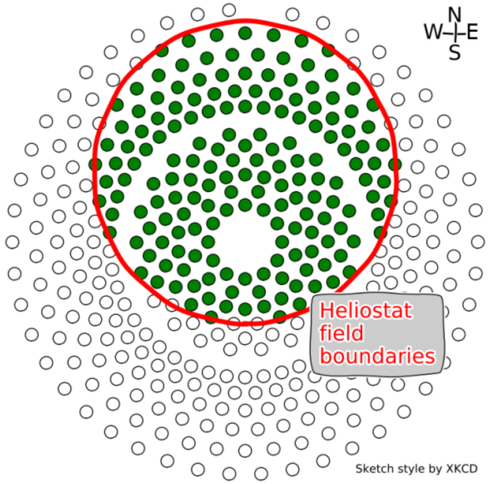

- Method: solar field heliostat selection based on polygon optimization and boundaries
- Coherent fields
- Area boundaries
- Flexible objective function

- ➢ Quantitative comparison to other approaches
- ➢ Allowable flux limits in objective function
- ➢ Area boundaries with undercuts, holes and hilly terrain

Ashalim Power Station, BrightSource Industries Israel (source: https://inhabitat.com/)

Thank you for your Attention!



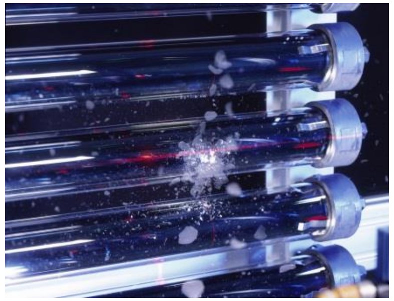
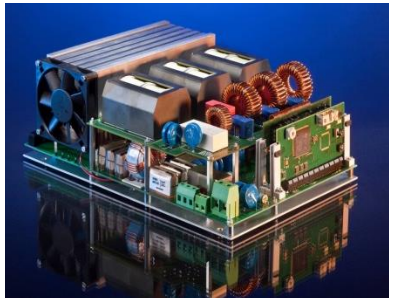
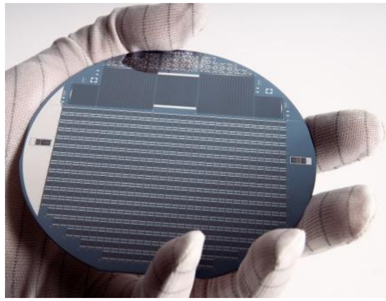


Fraunhofer Institute for Solar Energy Systems ISE

Shahab Rohani, Peter Schöttl

www.ise.fraunhofer.de

shahab.rohani@ise.fraunhofer.de
peter.schoettl@ise.fraunhofer.de

CASE STUDY

surrounding versus north fields

Heliostats fields, understanding the influence of latitude

AGENDA

- Interactive
  - Summer/winter solstice sun position
  - Calculation of cosine losses
- Latitude effects on surround/polar heliostat fields
  - Reference scenarios
  - Methodology recap
  - Result discussion

Summer/winter solstice sun position

- Location: Odeillo, France
- www.suncalc.org
- Summer (S) solstice: solar zenith $\theta_{s,S} = 19.1°$, solar elevation $\alpha_{s,S} = 70.9°$
- Winter (W) solstice: solar zenith $\theta_{s,W} = 65.9°$, solar elevation $\alpha_{s,S} = 24.1°$

Calculation of cosine losses

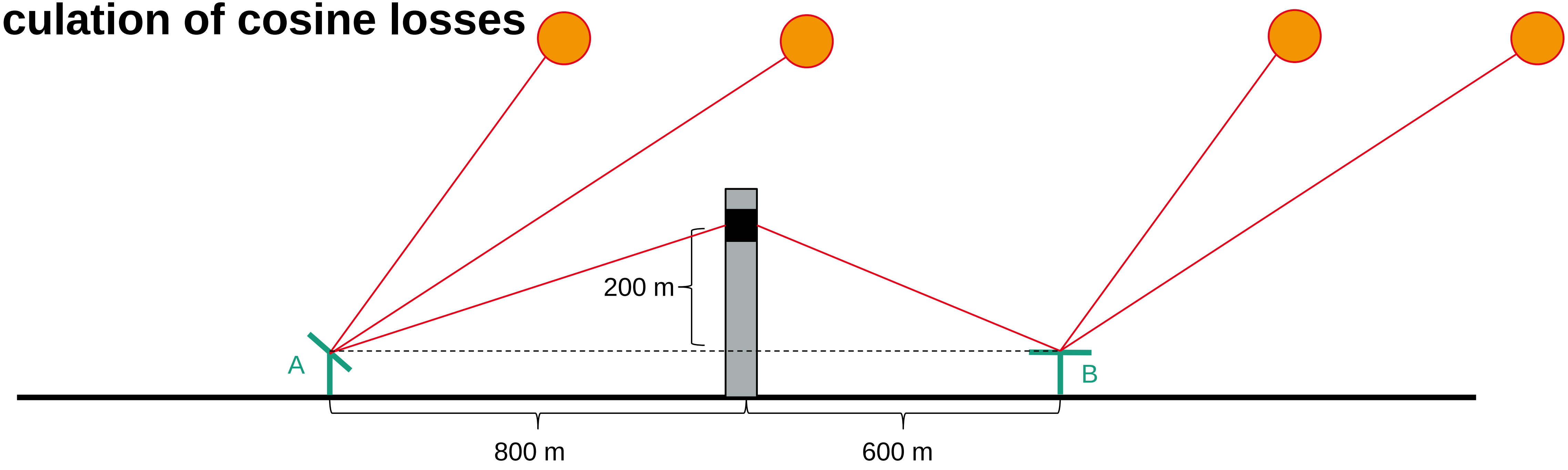

- Heliostat-tower angles: $\beta_A = \tan^{-1}\frac{200}{800} = 14.0°\,, \beta_B = \tan^{-1}\frac{200}{600} = 18.4°$
- Summer solstice: $\theta_{inc,A} = \frac{|\alpha_{s,S} - \beta_A|}{2} = \frac{|70.9° - 14.0°|}{2} = 28.5°, \theta_{inc,B} = \frac{|180° - \alpha_{s,S} - \beta_B|}{2} = 45.4°$
  Cosine losses: $1 - \cos\theta_{inc,A} = 0.12\,, 1 - \cos\theta_{inc,B} = 0.30$
- Winter solstice: $\theta_{inc,A} = 5.1°, \theta_{inc,B} = 68.8°$
  Cosine losses: $1 - \cos\theta_{inc,A} = 0\,, 1 - \cos\theta_{inc,B} = 0.64$

Reference scenarios

Sites

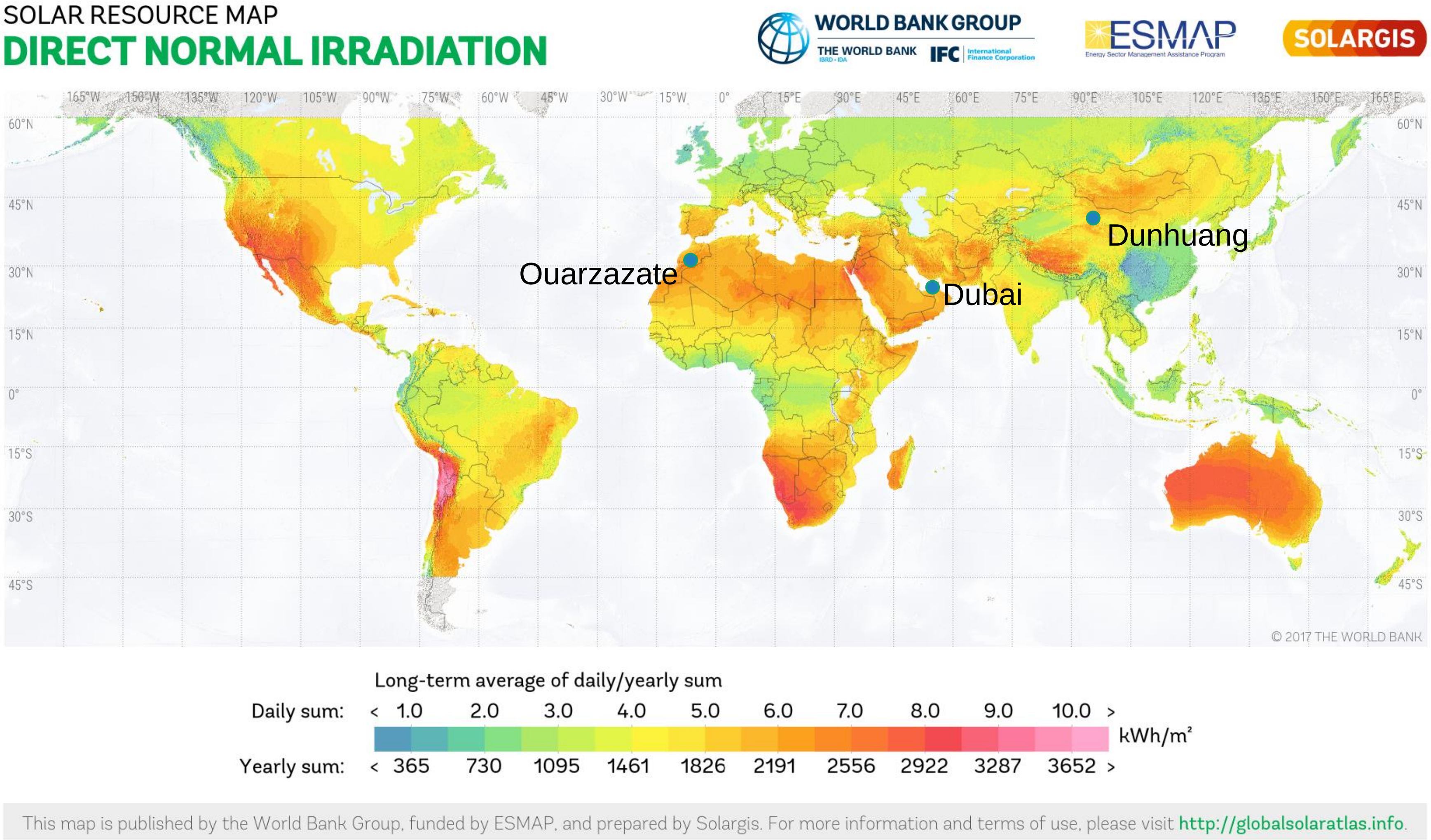

Reference scenarios
Parameters

	Dubai	Ouarzazate	Dunhuang
Location	24.8 °N, 55.4 °E	31.0 °N, 6.9 °W	39.8 °, 92.7 °E
Annual DNI	2.15 MWh/m²a	2.92 MWh/m²a	2.13 MWh/m²a
Design point DNI	800 W/m² at summer solstice		
Tower height	140 m		
Receiver design power	120 MW_{th}		
Receiver absorber area	521.5 m² (cavity), 260.8 m² (external)		
Heliostat mirror area	115.7 m²		
Heliostat beam quality	3 mrad		
Heliostat reflectance	93%		

Reference scenarios
External vs cavity

- Cavities combined with higher towers than external receivers
  - ignored
- Cavities larger than external receivers
  - $A_{abs,cavity} = A_{abs,external} \cdot 2$
  - Higher costs!

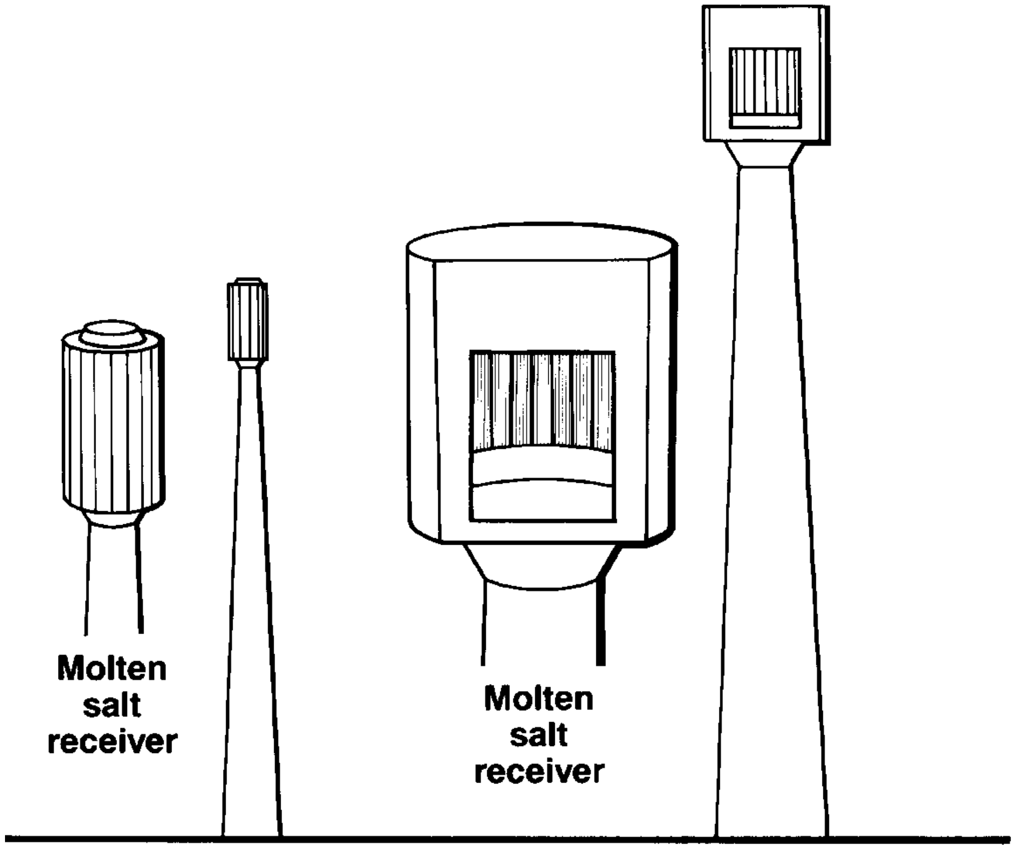

Source: P. K. Falcone, *A HANDBOOK FOR SOLAR CENTRAL RECEIVER DESIGN*. SAND-86-8009. Livermore, CA (USA), 1986.

Methodology recap

1. Create oversized MUEEN field
2. Assess heliostat annual efficiencies with Raytrace3D
3. Assess heliostat design point efficiencies with Raytrace3D
4. Select best-performing heliostats with polygon-based approach

Result discussion

Dubai: selected fields

Cavity

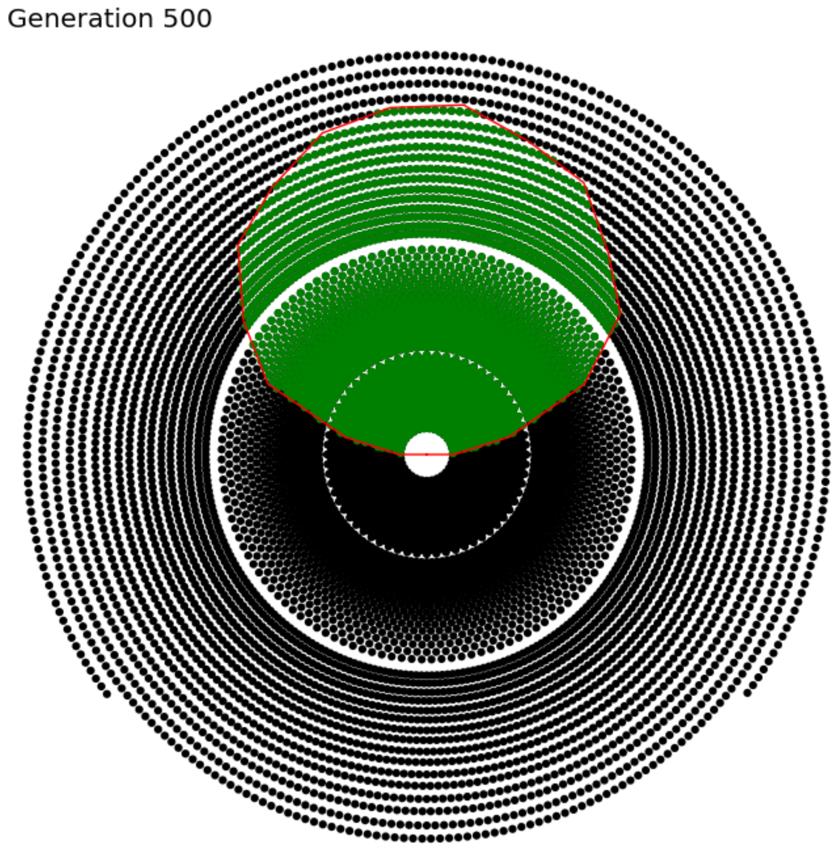

External

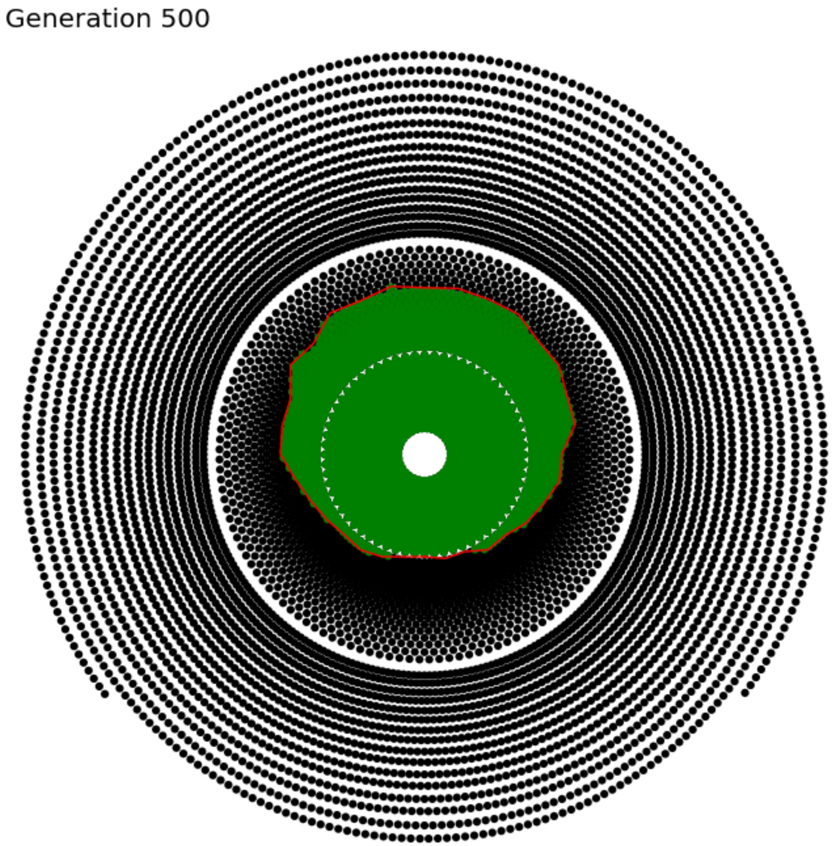

Result discussion

Ouarzazate: selected fields

Cavity

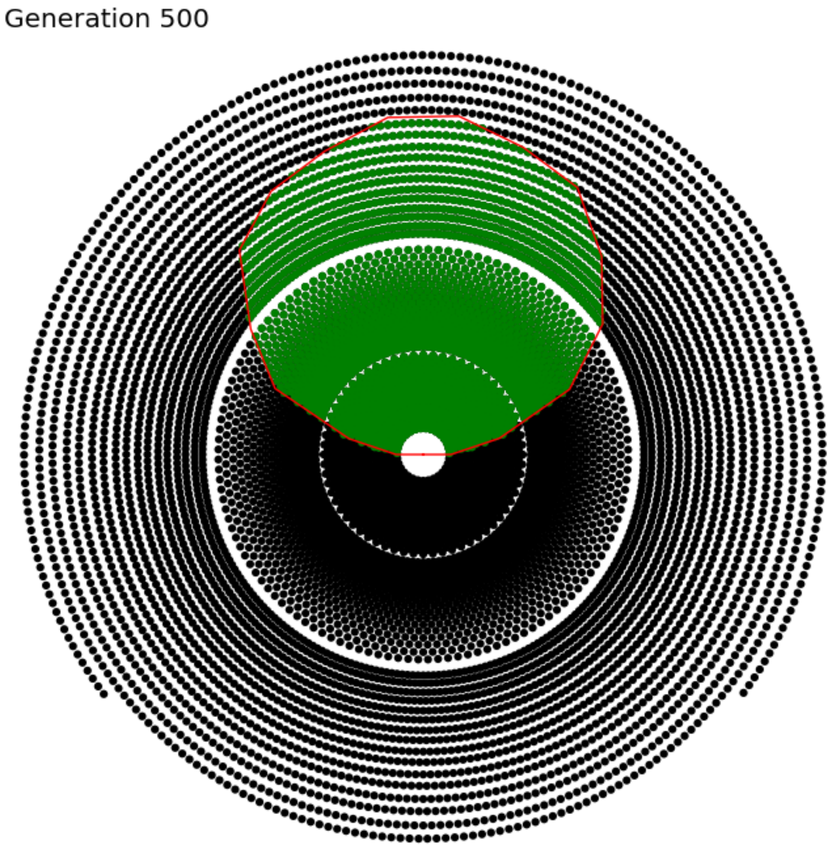

External

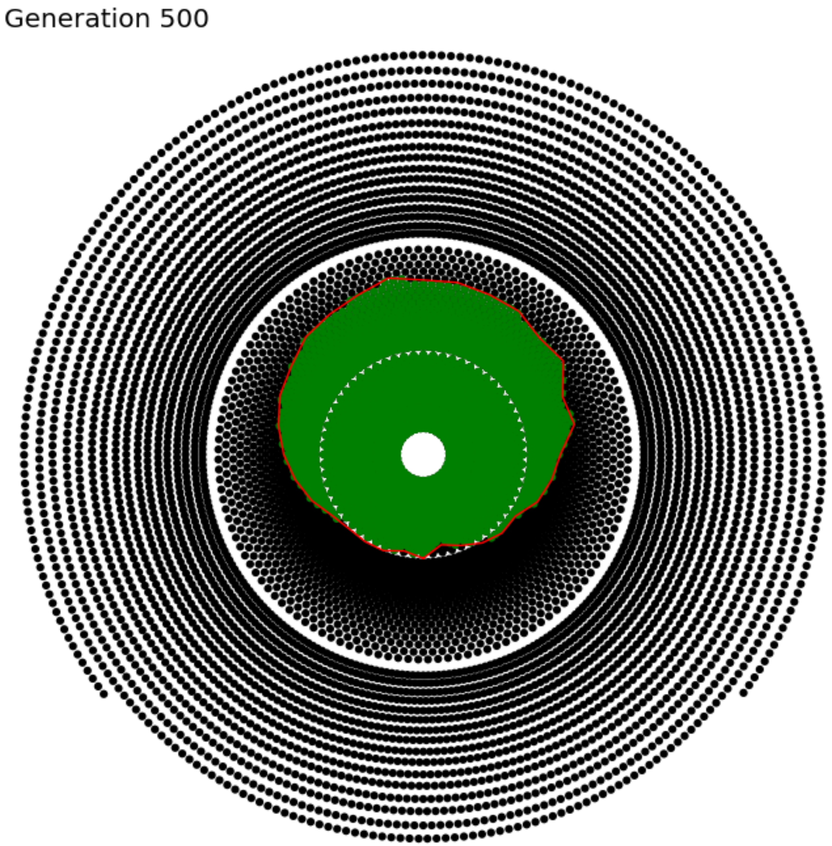

Result discussion

Dunhuang: selected fields

Cavity

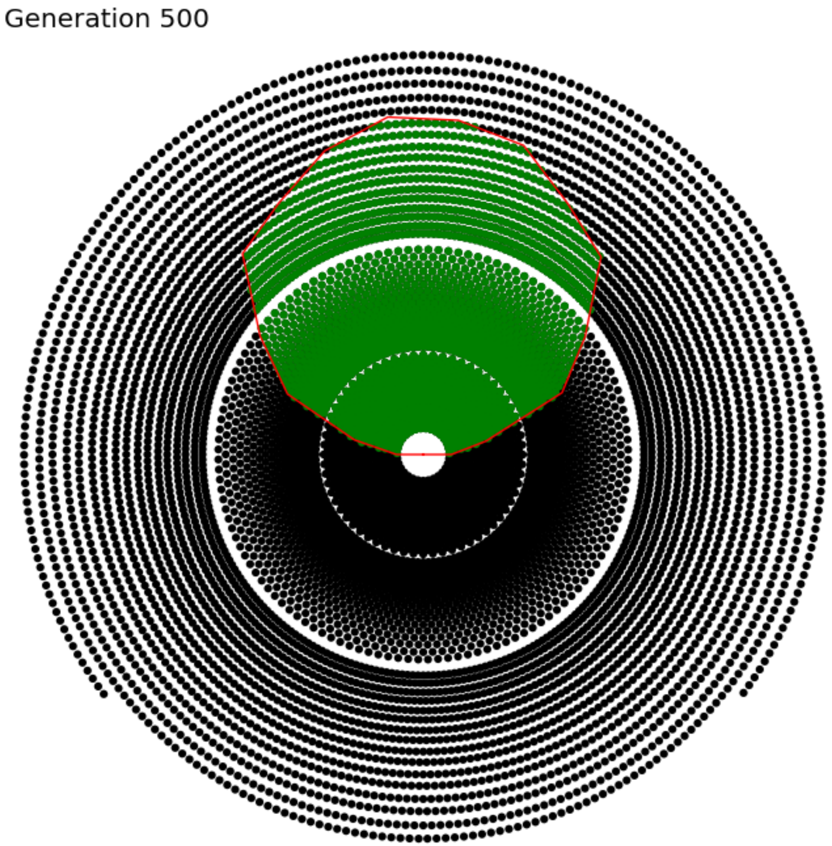

External

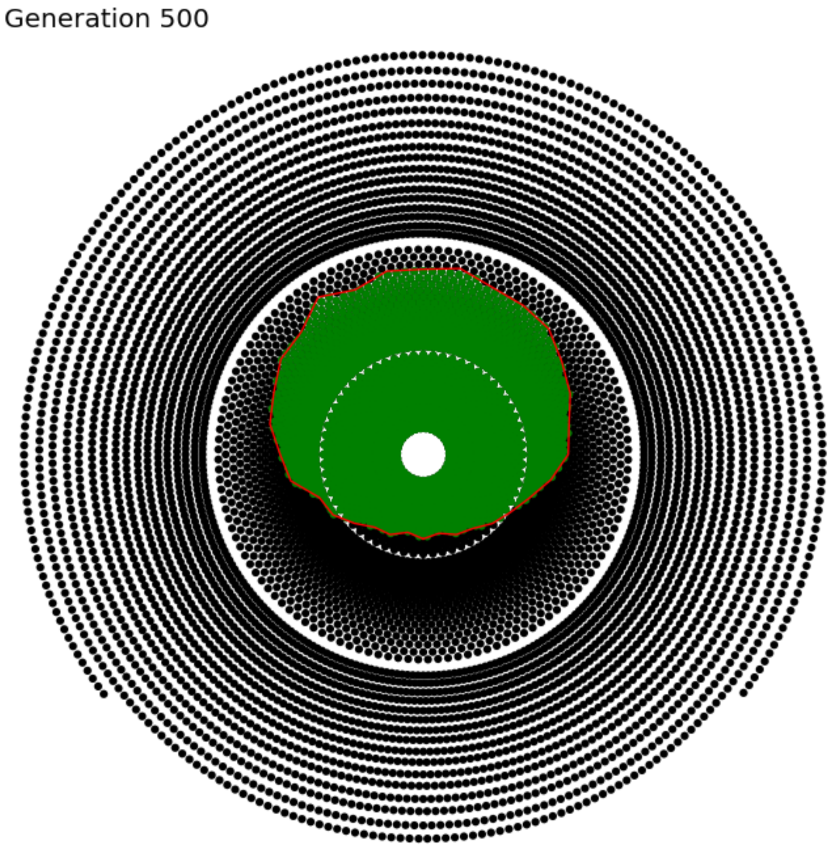

Result discussion

Dubai: optical losses

Cavity

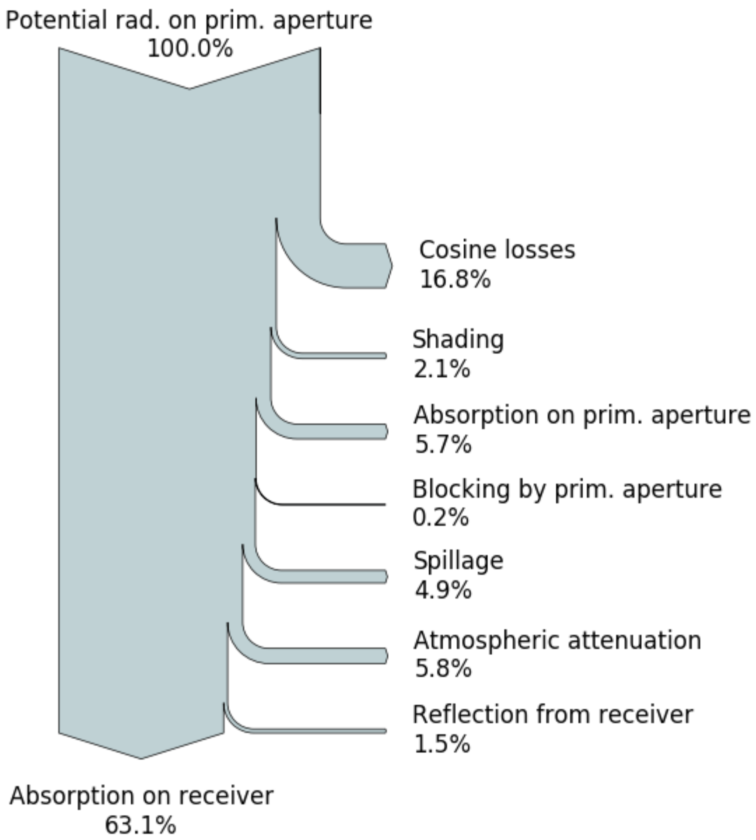

External

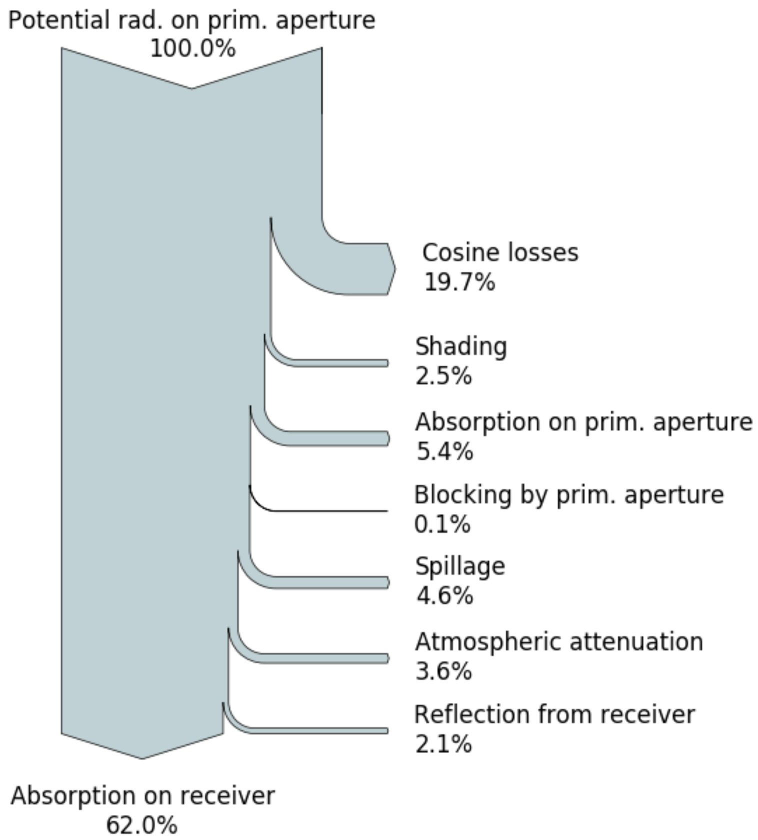

Result discussion

Ouarzazate: optical losses

Cavity

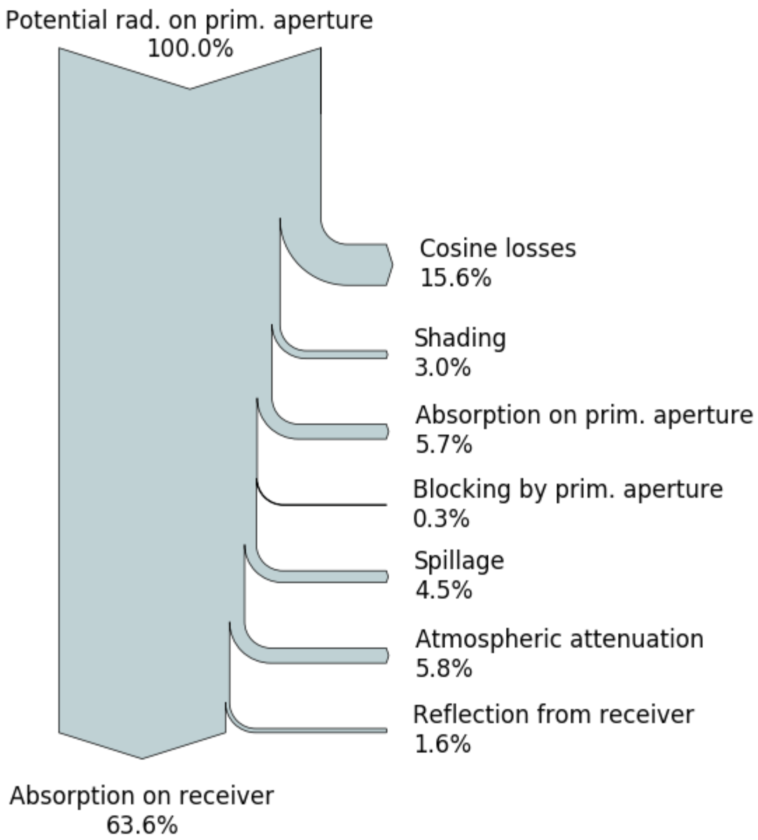

External

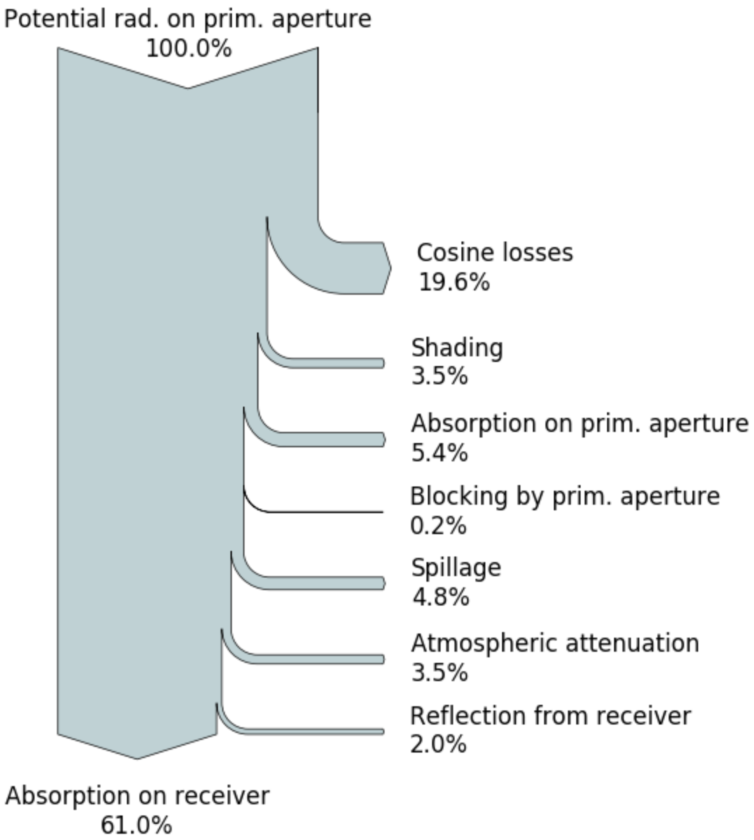

Result discussion
Dunhuang: optical losses

Cavity

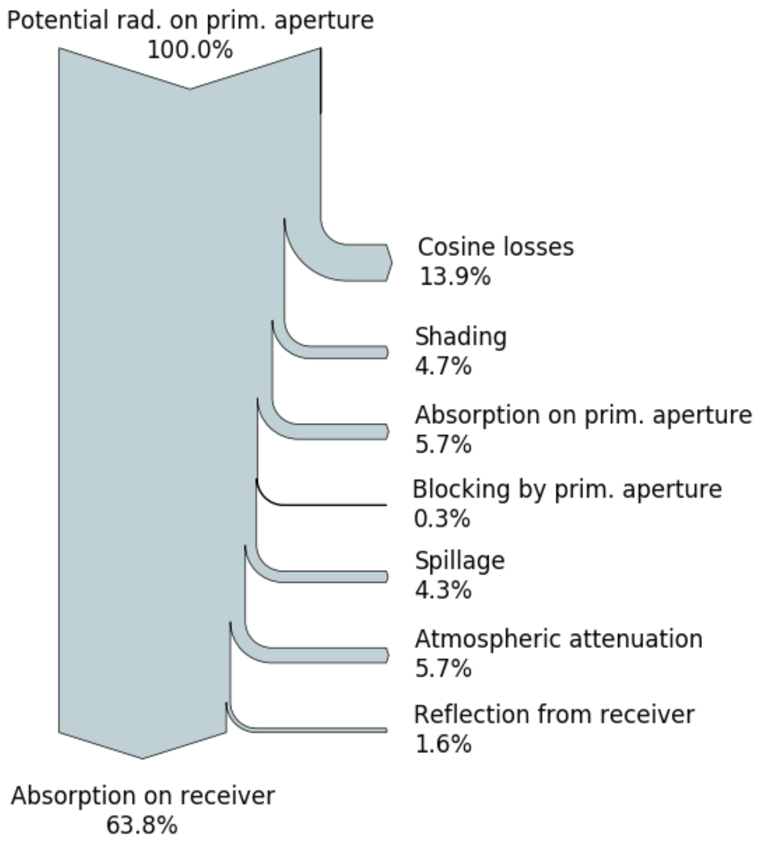

External

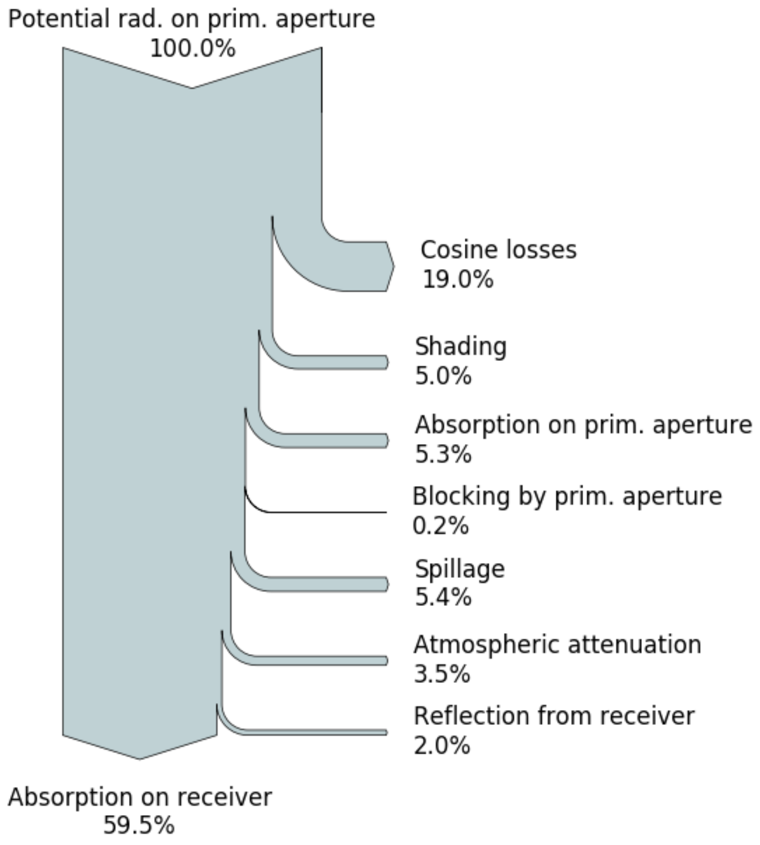

Result discussion
Summer/winter solstice

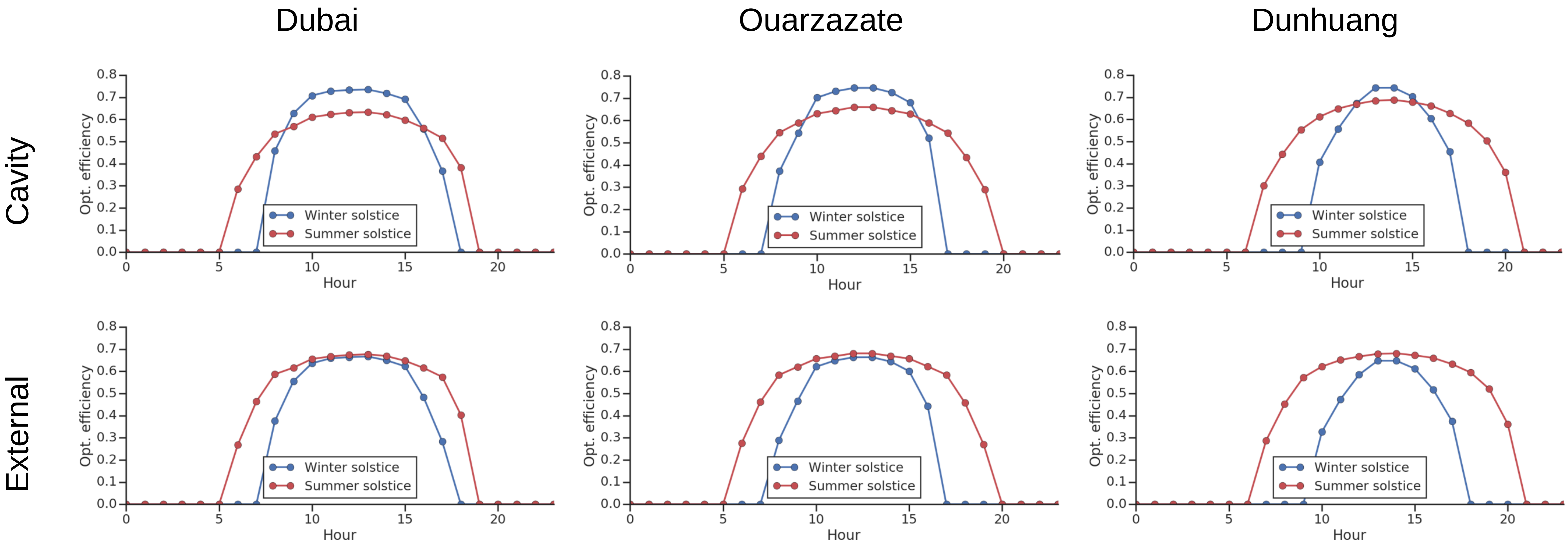

Result discussion
Annual optical efficiency

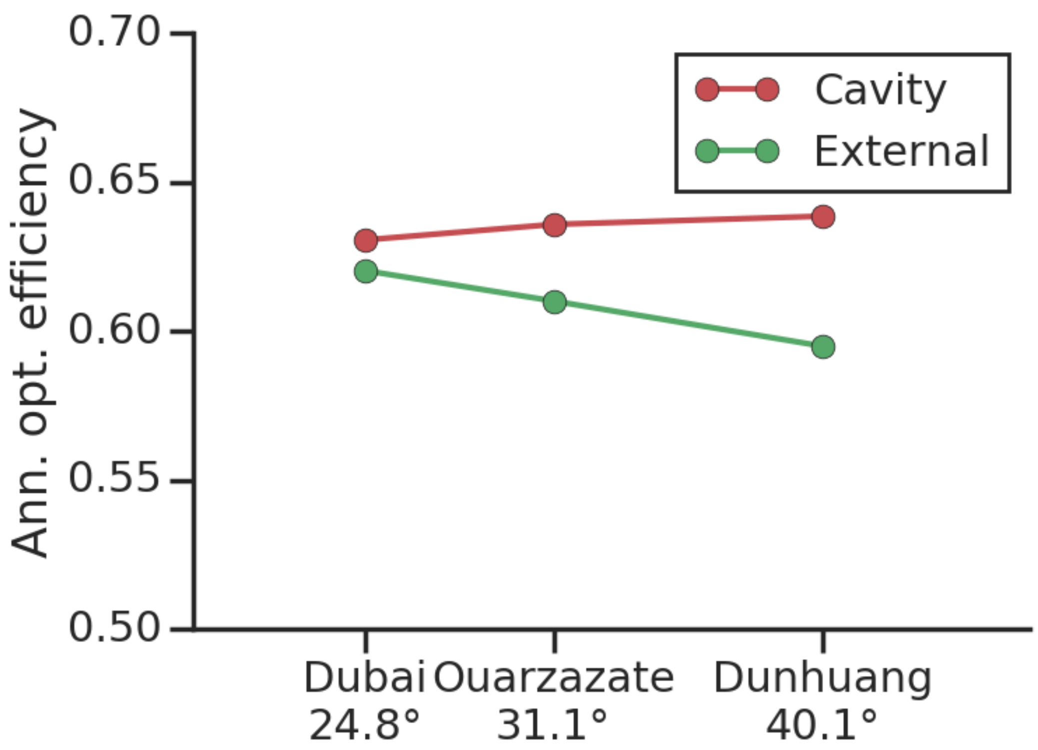

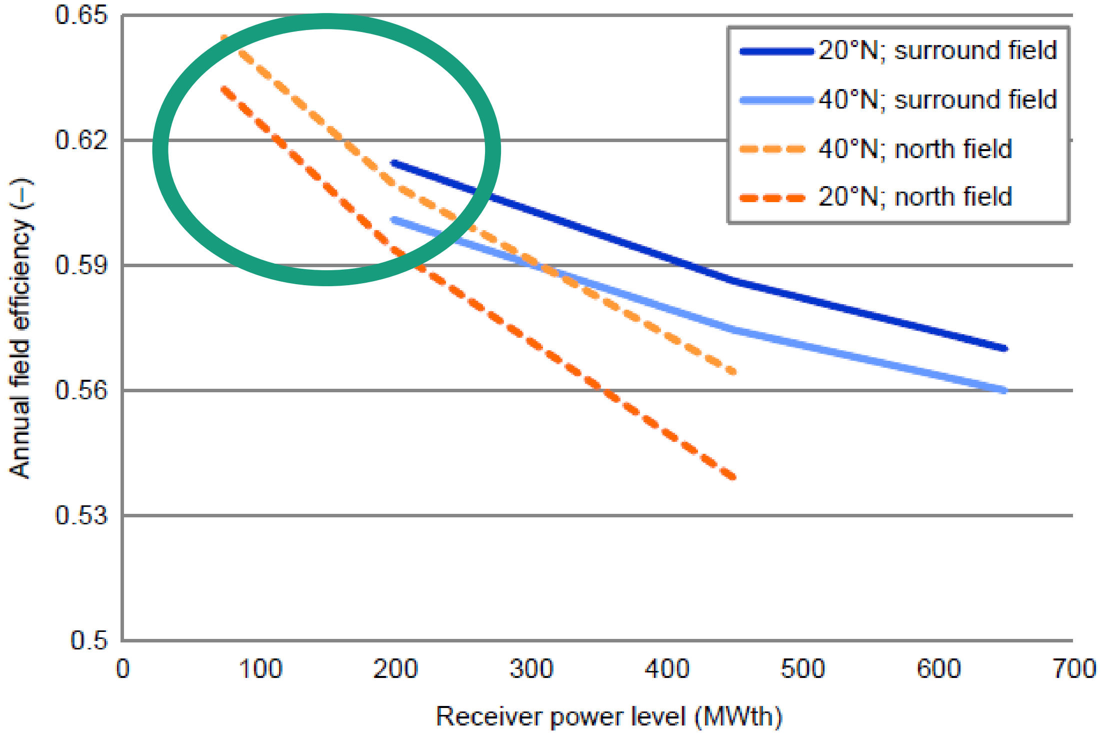

Source: R. Buck and P. Schwarzbözl, "4.17 Solar Tower Systems," in *Comprehensive Energy Systems*: Elsevier, 2018, pp. 692–732.

Thank you for your Attention!

  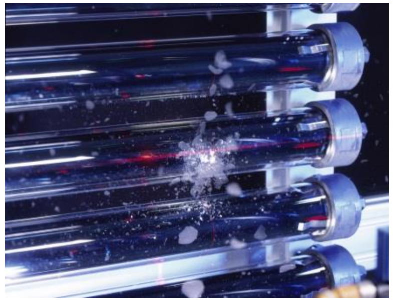 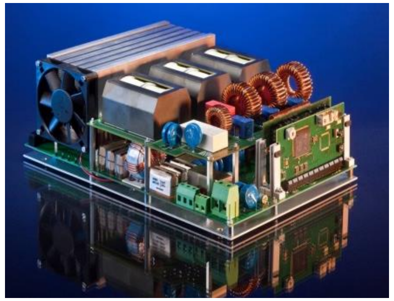 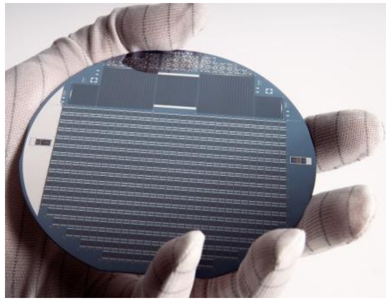 

Fraunhofer Institute for Solar Energy Systems ISE

Shahab Rohani, Peter Schöttl

www.ise.fraunhofer.de

shahab.rohani@ise.fraunhofer.de
peter.schoettl@ise.fraunhofer.de

Fraunhofer ISE